Numerical MSA solution for binary Yukawa mixtures

E. Arrieta, C. Jdrzejek, and K. N. Marsh

Citation: The Journal of Chemical Physics **86**, 3607 (1987); doi: 10.1063/1.451965
View online: http://dx.doi.org/10.1063/1.451965
View Table of Contents: http://scitation.aip.org/content/aip/journal/jcp/86/6?ver=pdfcov
Published by the AIP Publishing

Numerical MSA solution for binary Yukawa mixtures

E. Arrieta
Department of Chemical Engineering, Texas A&M University, College Station, Texas 77843

C. Jędrzejek[a)]
Center for Theoretical Physics, Department of Physics, Texas A&M University, College Station, Texas 77843

K. N. Marsh
Thermodynamics Research Center, Texas A&M University System, College Station, Texas 77843

(Received 25 November 1986; accepted 10 December 1986)

An efficient numerical algorithm is given to find the Blum and Høye mean spherical approximation (MSA) solution for binary mixtures of hard-core fluids with one-Yukawa interactions. The initial estimation of the variables is achieved by partial linearization (based on known, physical asymptotic behaviors) of the system of nonlinear equations which result from the Blum and Høye method. The complete procedure is at least one order of magnitude faster than that recently outlined by Giunta *et al.* More importantly, it always seems to converge to the physical solution (if it exists). We delimit, for several specific mixtures, the density-temperature region where no real solution is possible. This corresponds, following Waisman's interpretation, to thermodynamic conditions for which vapor–liquid or liquid–liquid separation occurs. The dependency of the MSA solutions on the Yukawa exponent z is studied in detail. For high values of z, adequate for generalized mean spherical approximation (GMSA) applications, we propose an accurate linear approximation, and we relate it to the solutions given by Giunta *et al.* For equal-sized, symmetric, equimolar binary mixtures, we show that Baxter's factorized version of the Ornstein–Zernike equation, including the factor correlation functions, can be decoupled. We also find, for equal-sized mixtures, that one of the approximations recently proposed by Jedrzejek *et al.* using an effective potential method is in very good agreement with our exact (MSA) results. Finally, a theoretical analysis shows that if the Yukawa amplitudes satisfy $K_{12} = \sqrt{K_{11}K_{22}}$, the coefficients D_{ij} of the factor correlation functions outside the core are related as follows: $D_{1i}/K_{1i} = D_{2i}/K_{2i}$, for $i = 1,2$.

I. INTRODUCTION

Progress in the theory of fluids depends on the availability of accurate analytic solutions that supplement the scarce computer simulation data. For liquid mixtures, Lebowitz[1] obtained a solution for additive hard spheres in the Percus–Yevick approximation. Another analytically solvable mixture is that composed of adhesive hard spheres.[2–4] This latter system is less interesting since it displays certain pathologies in its "critical" region, possibly due to the presence of a singularity in the potential. The most useful, analytically solvable system representing a qualitatively realistic mixture, however, is that of hard cores with attractive Yukawa tails. For this case, Blum and Høye (BH)[5] gave a formal solution, within the mean spherical approximation (MSA), based on Baxter's factorization[6] of the Ornstein–Zernike equation. A similar solution, but using the Laplace transform method,[7,8] is due to Niizeki.[9]

Blum and Høye's equations are restricted to the Yukawa exponent z being equal for all intercomponent interactions. In 1980, the BH solution was generalized for pair-specific z_{ij} by Cummings,[10] and Cummings and Smith.[11] These authors found a numerical solution, through a laborious procedure, for the coefficients of the factor correlation functions $Q_{ij}(r)$ [auxiliary functions from which both the total, $h_{ij}(r)$, and direct, $c_{ij}(r)$, correlation functions can be computed] for one particular example. However, they did not calculate any thermodynamic or structural properties. Recently Giunta, Abramo, and Caccamo[12] obtained numerical results for a binary Yukawa mixture using the BH equations. Following the generalized mean spherical approximation (GMSA),[13] they assumed a Yukawa form, with large values of z, for the direct correlation functions in order to improve structural calculations for hard-sphere mixtures. As it will be seen in Sec. V, this presents one of the most favorable cases to solve the system of nonlinear equations resulting from the BH method, for it becomes almost linear. Based on this, we will examine their results.

We extend here the work of Giunta *et al.* Specifically, we provide a much faster, direct (as opposed to stepwise) solution procedure, we completely determine the dependency of the solutions on the Yukawa exponent z, and provide analytic expressions for all MSA thermodynamic properties. The quantitative knowledge of such properties is of considerable interest for several reasons:

(1) The hard core with Yukawa tail potential has a screened Coulomb form[14] and, therefore, is directly applicable to the study of liquid metals. [Previously available solution methods required all components to have the same size and were based on the decoupling of the number density and concentration fluctuations, $S_{NC}(0) = 0$, which for strongly ordering systems leads to physically unrealistic results.]

(2) The Yukawa mixture, used in the context of the

[a)] On leave from Department of Physics, Jagellonian University, Cracow, Poland.

 0021-9606/87/063607-20$02.10

GMSA, can serve as a means of improvement of the *PY* solution for hard-sphere mixtures.

(3) Mixtures with a Yukawa potential can serve as a better reference system for perturbation methods than either hard-sphere mixtures of Lennard-Jones pure components combined according to available mixing rules.

We present a complete and efficient numerical algorithm for solving the BH equations for binary mixtures. Section II develops those equations to their final form: a system of nonlinear equations. The solution procedure is shown in Sec. III. Its most important aspect is the initial estimation of the variables, obtained by partial linearization of the nonlinear equations. In all cases investigated, this algorithm converged to the physical solution (if it existed). We delimit, for several mixtures, the ρ, T region where no (real) mathematical solutions exist for the BH equations. In Sec. IV we calculate the coefficients of the $Q_{ij}(r)$ functions from which the $c_{ij}(r)$ and $h_{ij}(r)$ correlation functions, and hence all structural properties, can be easily computed. Section IV also gives analytic expressions for the MSA thermodynamic properties.

Section V determines the dependency of the BH solution on the Yukawa exponent z, especially at large values of this parameter. For that case, we obtain a very accurate approximate solution by expanding the equations on $1/z$ and neglecting second and higher order terms. We use this approximation to reexamine the recent GMSA results by Giunta *et al.*[12]

Section VI concentrates on mixtures of equal-sized components. For the symmetric (equal like-particle interactions for both components), equimolar ($x_1 = x_2 = 0.5$) case, we show that Baxter's factorized version of the Ornstein–Zernike equation can be decoupled into two parts, each one describing a hypothetical pure component. We also use our exact MSA results to evaluate two recent approximations proposed by Jedrzejek *et al.*[15]

Section VII presents a summary of conclusions and addresses some immediate applications. In addition, a theoretical analysis in Appendix D shows that when the crossed interactions satisfy $K_{12} = \sqrt{K_{11}K_{22}}$ (see the next section), the coefficients D_{ij} of the factor correlation functions outside the core relate themselves in pairs according to $D_{1i}/K_{1i} = D_{2i}/K_{2i}$, for $i = 1,2$. We also extend this result to multicomponent mixtures and examine the significance of this intrinsic characteristic of the BH equations.

II. BLUM AND HØYE'S MSA EQUATIONS FOR YUKAWA MIXTURES

The interaction potential for a mixture of hard spheres of diameter σ_i with a one-Yukawa tail outside the core is

$$\phi_{ij}(r) = \begin{cases} \infty & \text{for } r < \sigma_{ij} \\ -\sigma_{ij}\epsilon_{ij}\dfrac{e^{-z(r-\sigma_{ij})}}{r} & \text{for } r \geqslant \sigma_{ij} \end{cases}, \tag{1}$$

where $\sigma_{ij} = \frac{1}{2}(\sigma_i + \sigma_j)$ (the additive hard-core assumption), ϵ_{ij} are the magnitudes of the interactions at the hard-core distances and the Yukawa exponent, or inverse range parameter, z is common for all i,j pairs.

In the mean spherical approximation (MSA) the Ornstein–Zernike (OZ) equation for mixtures,

$$h_{ij}(r) = c_{ij}(r) + \sum_l \rho_l \int c_{il}(s) h_{lj}(|\mathbf{r} - \mathbf{s}|) d\mathbf{s}, \tag{2}$$

is given the following two-part closure,

$$h_{ij}(r) = -1 \quad \text{for } r < \sigma_{ij}, \tag{3}$$

$$c_{ij}(r) = K_{ij}\frac{e^{-z(r-\sigma_{ij})}}{r} \quad \text{for } r \geqslant \sigma_{ij}, \tag{4}$$

where

$$K_{ij} = \frac{\sigma_{ij}\epsilon_{ij}}{kT}. \tag{5}$$

In these equations, $h_{ij}(r) = g_{ij}(r) - 1$ are the total correlation functions (TCF), $g_{ij}(r)$ are the two-body radial distribution functions (RDF) between particles of species i and j, and $c_{ij}(r)$ are the direct correlation functions (DCF). The densities of the components in the mixture is represented by ρ_i. In Eq. (5) k is Boltzmann's constant and T is the temperature. One can also disregard Eq. (5) and treat Eqs. (3) and (4) as a generalized mean spherical approximation (GMSA) closure to improve the PY solution for hard-sphere mixtures.

To calculate the thermodynamic properties of this mixture, the total number density ρ, composition x_i (or, alternatively, the number densities of the components $\rho_i = \rho x_i$), and temperature T must be specified.

We will use Baxter's factorized version[6] of the OZ equation for mixtures as given by Blum and Høye[5]:

$$2\pi r c_{ij}(r) = -Q'_{ij}(r) + \sum_l \rho_l \int_{\lambda_{lj}}^{\infty} Q_{jl}(t) Q'_{il}(r+t) dt, \tag{6}$$

$$2\pi r h_{ij}(r) = -Q'_{ij}(r) + 2\pi \sum_l \rho_l \int_{\lambda_{jl}}^{\infty} (r-t) \times h_{il}(|r-t|) Q_{lj}(t) dt, \tag{7}$$

where $\lambda_{ji} = \frac{1}{2}(\sigma_j - \sigma_i)$, the range of the interaction potential has been extended to infinity, and $Q_{ij}(r)$ are the factor correlation functions (FCF), $Q'_{ij}(r)$ being their derivatives. Thus, for n-component mixtures, we have two sets of n^2 equations each; Eqs. (6) and (7), in $3n^2$ functional unknowns: $\{c_{ij}(r)\}$, $\{h_{ij}(r)\}$, and $\{Q_{ij}(r)\}$. The additional set of n^2 equations needed to make the problem solvable is provided by Eq. (3) within the core, and by Eq. (4) outside it.

From Eqs. (6) and (7) subject to the conditions given by Eqs. (3) and (4), $Q_{ij}(r)$ must have the following form:

$$Q_{ij}(r) = Q^0_{ij}(r) + \frac{1}{z} D_{ij} e^{-z(r-\sigma_{ij})}, \tag{8}$$

where

$$(Q_{ij}^{0}(r) = \begin{cases} \frac{1}{2}a_{ij}(r-\sigma_{ij})^2 + b_{ij}(r-\sigma_{ij}) + \frac{1}{z}C_{ij}(e^{-z(r-\sigma_{ij})}-1) & \text{for } \lambda_{ji} < r < \sigma_{ij} \\ 0 & \text{for } r \geq \sigma_{ij} \end{cases} \quad (9)$$

This expression is a slight modification of that used by Blum and Høye, the correspondence being

$$a_{ij} = (q_{ij}'')_{\mathrm{BH}} ,$$
$$b_{ij} = (q_{ij}')_{\mathrm{BH}} ,$$
$$C_{ij} = ze^{-z\sigma_{ij}}(C_{ij})_{\mathrm{BH}} ,$$
$$D_{ij} = ze^{-z\sigma_{ij}}(D_{ij})_{\mathrm{BH}} , \quad (10)$$

where the two changes of variables affecting the exponential terms were introduced for numerical convenience, especially at high values of the Yukawa exponent z.

There are, in principle, four sets of unknowns: the coefficients of the $Q_{ij}(r)$. Besides, when we perform the integrations involving the unknown function $h_{ij}(r)$, or equivalently $g_{ij}(r)$, we create one more set of unknowns, denoted by

$$\hat{g}_{ij} = \hat{g}_{ij}(z) = \int_0^\infty r e^{-zr} g_{ij}(r) dr . \quad (11)$$

As a result, five sets of quantities must be found to solve the problem:

$$\{a_{ij}\},\{b_{ij}\},\{C_{ij}\},\{D_{ij}\},\{\hat{g}_{ij}\} .$$

Using Eqs. (7) within the core, together with Eq. (3), for the left-hand side and Eqs. (8) and (9) for the right-hand side, one gets three kinds of terms: terms in r, constant terms, and exponential terms. Equating both sides of Eq. (7) for each of these kinds, three sets of n^2 equations are obtained. They permit $\{a_{ij}\}$, $\{b_{ij}\}$, and $\{C_{ij}\}$ to be expressed as functions of $\{D_{ij}\}$ and $\{\hat{g}_{ij}\}$. Consequently, the problem is reduced to the determination of these two last sets of unknowns from two sets of equations, Eqs. (6) and (7), both for $r \geq \sigma_{ij}$.

However, the direct use of Eq. (7) presents some mathematical inconvenience. It is better to take Eq. (7) for $r < \sigma_{ij}$, extend it analytically outside the core, and substract it from the original version of Eq. (7). After Laplace transformation, the application of the convolution theorem allows us to separate the integral in Eq. (7) into the product of two integrals (one of them yielding $\hat{g}_{ij}$).

Blum and Høye[5] explain fully the procedure we have just recapitulated. Following it, the entire problem can be described by a system of $2n^2$ nonlinear equations in $2n^2$ unknowns, n being the number of components in the mixture. (Note that these authors' article contains a few typographical errors which we list in Appendix A.) Once BH's method has been completely developed, we find that the final system can be divided into two subsets of n^2 equations each:

$$\sum_{lmk} A_{kmjl}^{(1)} G_{mk} D_{kl} D_{il} + \sum_{lk} A_{kjl}^{(2)} D_{kl} D_{il} + \sum_{i} A_{ij}^{(3)} D_{il} + A_{ij}^{(4)} = 0 , \quad (12)$$

$$\sum_{lmk} B_{mlkj}^{(1)} G_{il} G_{km} D_{mj} + \sum_{lmk} B_{kmlij}^{(2)} G_{kl} D_{mj} + \sum_{m} B_{mij}^{(3)} D_{mj} + \sum_{m} B_{mj}^{(4)} G_{im} + B_{ij}^{(5)} = 0 , \quad (13)$$

All subindices vary between 1 and n. The $A^{(\gamma)}$ and $B^{(\gamma)}$ parameters can be calculated from the data σ_i, ϵ_{ij}, z, ρ_i, T. Appendix B gives explicit expressions for their determination. The only unknown quantities are the $\{D_{ij}\}$ coefficients of the factor correlation functions and the transforms $\{G_{ij}\}$ whose relation to the radial distribution functions is given by

$$G_{ij} = z\hat{g}_{ij} e^{z\sigma_{ij}} = z\int_{\sigma_{ij}}^\infty r e^{-z(r-\sigma_{ij})} g_{ij}(r) dr . \quad (14)$$

This change of variable permits us to eliminate most exponentials (and in particular all which have a positive exponent) when calculating the parameters of Eqs. (12) and (13).

III. SOLUTION PROCEDURE FOR BINARY MIXTURES

To determine the (MSA) properties of a binary Yukawa mixture we must solve the system of eight nonlinear equations in eight unknowns $\{D_{ij}\}$, $\{G_{ij}\}$ represented by Eqs. (12) and (13). This is the only nonanalytical part of the problem.

The efficiency of iterative methods to solve systems of nonlinear equations is greatly affected by the way the equations are written. We find that Eqs. (12) and (13) constitute a well-behaved system when the Newton–Raphson technique is used, with the partial derivatives evaluated analytically.

As a measure of the error for any set of the variables, the following norm of the deviations is used:

$$\Omega = \sqrt{\frac{1}{8}\sum_{ij}\left\{\left[\frac{\Theta_{ij}^{(a)}}{\max(1, A_{ij}^{(4)})}\right]^2 + \left[\frac{\Theta_{ij}^{(b)}}{\max(1, B_{ij}^{(5)})}\right]^2\right\}} , \quad (15)$$

where $\Theta_{ij}^{(a)}$ and $\Theta_{ij}^{(b)}$ are the deviations from zero for the left-hand side of Eqs. (12) and (13), respectively. A tolerance $\Omega < 10^{-6}$ is small enough to uniquely determine the first six significant digits for all thermodynamic properties.

At every Newton–Raphson iteration we check the above norm of the error to avoid overshooting. However, no limits (which would be quite difficult to choose for the $\{D_{ij}\}$) are imposed on the variables. Our initial estimate (see below) ensures that the variables will remain within the physically acceptable region.

Since our system of equations is composed of two subsystems, Eqs. (12) and (13), which are linear in the $\{G_{ij}\}$ and $\{D_{ij}\}$ sets of variables, respectively, we can express one of these sets in terms of the other and reduce the system to

TABLE I. Molecular characteristics of the mixtures used in this work.

Mixture designation	σ_2/σ_1	ϵ_{11}[a]	ϵ_{12}	ϵ_{22}	$z\sigma_1$
M1	1.500	1.000	0.800	0.900	1.800
M2[b]	1.167	1.000	$\sqrt{\epsilon_{11}\epsilon_{22}}$	1.919	1.800

[a] All ϵ_{ij} scaled by $|\epsilon_{11}|$.

[b] The ratios σ_2/σ_1 and $\epsilon_{22}/\epsilon_{11}$ for this M2 mixture are equal to those for the Lennard-Jones potential of argon (1) and xenon (2) (Ref. 16).

four equations in four unknowns. We achieved this using SMP (symbolic manipulation program). However, the application of a standard subroutine for solving nonlinear equations to the reduced system resulted in a highly unstable iterative procedure.

Another way of exploiting the mentioned linearity is to apply the Newton–Raphson method to just one of the subsystems, say Eq. (12) in the $\{G_{ij}\}$, with the accompanying $\{D_{ij}\}$ being linearly calculated from the other subsystem. We found that, except for very good initial guesses, these schemes tend to "derail" the variables to regions of no convergence or, more rarely, to unphysical solutions.

In order to provide numerical results, we will use two specific mixtures, M1 and M2, whose molecular characteristics are described in Table I.

For some conditions, Eqs. (12) and (13) lack real solutions. In Figs. 1 and 2 we delimit the region in the packing fraction, $\eta = (\pi/6)\ \Sigma_i\ \rho_i\sigma_i^3$, reduced temperature $T^* = kT/|\epsilon_{11}|$, plane where no real solution is possible for mixtures M1 and M2 at several compositions. Following Waisman's[8] interpretation, we conclude that under such conditions phase separation occurs. While mixture M2, which is close to ideal, exhibits vapor–liquid separation only, M1 can also undergo a liquid–liquid separation (second positive slope). This is because the unlike-particle attractions (ϵ_{12}) in M1 are weaker than either of the like-particle interactions (ϵ_{11},ϵ_{22}). In addition, Fig. 1, especially at $x_1 = 0.65$, underlines the continuity between liquid–liquid and gas–gas equilibrium.

The curves in Figs. 1 and 2 (absence of real solutions) do not have a strict physical meaning. However, they are truly indicative of phase transitions. Enclosing their vapor–liquid part, there must lie a curve of mechanical instability. Further out (at higher temperatures), we should find a material instability curve surrounding both vapor–liquid and liquid–liquid regions. Lastly, two-phase calculations would define the coexistence curve around all the previous ones (except at the critical point where it touches the region of material instability). We leave their determination for a future paper.

A. Initial estimation

An essential part in any iterative method is the initial estimation of the solution. For our problem, earlier workers[11,12] solved this question through a stepwise variation of the data. Starting from some known solution (pure component i at fixed ρ_i in the case of Cummings and Smith,[11] hard-sphere mixture for Giunta *et al.*[12]) they change some data (ρ_j and T, respectively) by small steps until the conditions of interest are reached. At each step, the final solution from the previous one is taken as the initial guess.

In contrast, we work directly with the thermodynamic conditions of interest. Our initial estimate is derived from the analysis of three asymptotic cases, each yielding a unique, physical solution: infinite temperature T, zero density ρ, and infinite value of the Yukawa exponent (or inverse range parameter) z.

With regard to the first limit case, it is worth noting that all energy-related quantities, ϵ_{ij} and T, take part in the sys-

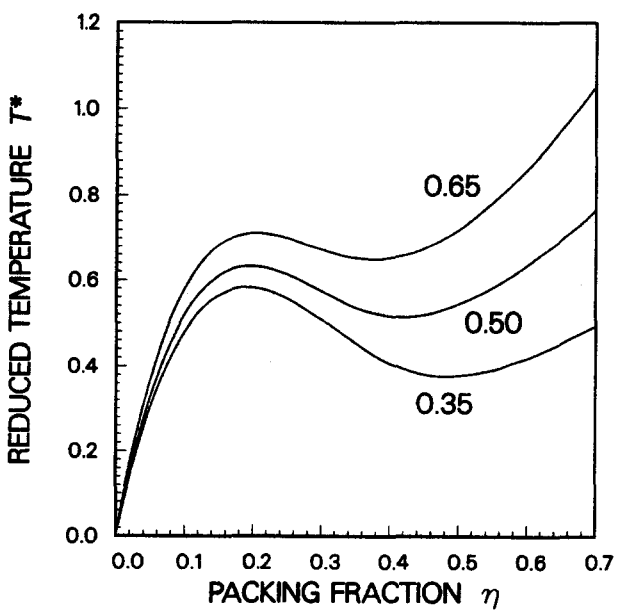

FIG. 1. Region (below the curves) of nonreal mathematical solution for M1 mixtures at different compositions x_1. The reduced temperature is given by $T^* = kT/|\epsilon_{11}|$.

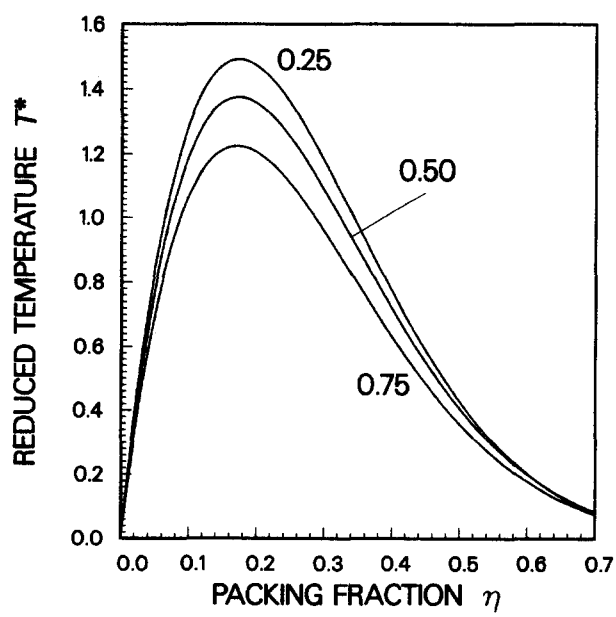

FIG. 2. Same as Fig. 1 for M2 mixtures.

tem only through the coefficients $A_{ij}^{(4)}$ [see Eq. (5) and Appendix B]. Therefore, at *infinite temperature* the $A_{ij}^{(4)}$ parameters vanish and hence all D_{ij} are driven to zero. This is in accordance with the known fact that, in the MSA, the factor correlation functions $Q_{ij}(r)$ disappear outside the molecular core [Eq. (8)] for hard spheres. Taking this result to Eq. (13) we get the following linear system:

$$\sum_m B_{mj}^{(4)} G_{im} = -B_{ij}^{(5)} . \tag{16}$$

This yields the exact $\{G_{ij}\}$ solution for the corresponding hard-sphere mixture. Since the radial distribution functions are mainly determined by the hard cores, this approximation is excellent. However, taking the $\{D_{ij}\}$ equal to zero gives rise to a rather poor guess at normal temperatures. Instead, we assume that they are just small. Thus, neglecting the second order terms in Eq. (11) another linear system results:

$$\sum_l A_{lj}^{(3)} D_{il} = -A_{ij}^{(4)} . \tag{17}$$

Equations (16) and (17) constitute our type 1 estimate and they produce a good approximation.

For both the other two limit cases, *zero density* and *infinite z*, the formulas in Appendix B indicate that the coefficients $A^{(1)}$, $A^{(2)}$, $B^{(1)}$, and $B^{(2)}$ become zero. Based on this, we can, for any values of ρ and z, neglect the corresponding terms and use the remaining linear system to obtain an initial estimate:

$$\sum_l A_{lj}^{(3)} D_{il} = -A_{ij}^{(4)} , \tag{18}$$

$$\sum_m B_{mj}^{(4)} G_{im} = -B_{ij}^{(5)} - \sum_m B_{mij}^{(3)} D_{mj} , \tag{19}$$

where the D's in the second equation are those obtained from the first. This alternative estimation, which we call type 2, gives, obviously, the same set of $\{D_{ij}\}$ as the previous one. At low, vapor-like, densities and, more importantly, high values of z, such as those used by Giunta *et al.* in GMSA applications, it produces better estimates than type 1. [In relation to the latter case, it is worth noting that Eqs. (18) and (19) contain all terms in z^0 and z^{-1} present in the full system.] In general, however, this estimation is less satisfactory than that coming from Eqs. (16) and (17); one of the reasons being that Eq. (19) yields $G_{12} \neq G_{21}$. Under demanding conditions—high densities, very low temperatures, and near phase separation—this may lead to unphysical solutions.

The strengths of both estimates can be combined in the following direct iteration scheme:

$$\left(\sum_l A_{lj}^{(3)} D_{il}\right)_{\alpha+1} = -\left(\sum_{lmk} A_{kmjl}^{(1)} G_{mk} D_{kl} D_{il} + \sum_{lk} A_{kjl}^{(2)} D_{kl} D_{il} + A_{ij}^{(4)}\right)_{\alpha} , \tag{20}$$

$$\left(\sum_m B_{mj}^{(4)} G_{im}\right)_{\alpha+1} = -\left(\sum_{lmk} B_{mlkj}^{(1)} G_{il} G_{km} D_{mj} + \sum_{lmk} B_{kmlij}^{(2)} G_{kl} D_{mj} + \sum_m B_{mij}^{(3)} D_{mj} + B_{ij}^{(5)}\right)_{\alpha} , \tag{21}$$

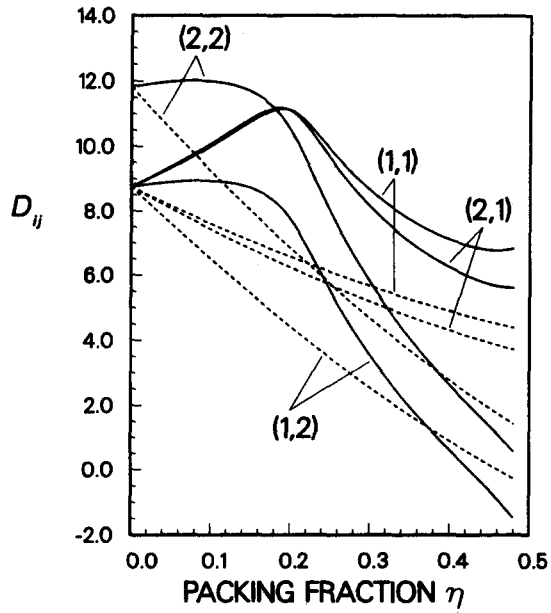

FIG. 3. Comparison between initial estimates and solution values for the $\{D_{ij}\}$ for mixture M1 at $x_1 = 0.65$ and temperature $T^* = 0.717$. The solid lines represent the solution values and the dashed lines are the results yielded by both types of estimate.

where the subindices outside the parenthesis refer only to the variables. At $\alpha = 0$ all variables are taken equal to zero, recovering Eqs. (17) and (16). In many cases the final solution can be reached through this procedure in a reasonable number of iterations. However, this direct substitution scheme requires more computer time than the Newton–Raphson method unless the thermodynamic conditions approach any of the three limit cases discussed previously.

Figures 3 to 8 evaluate both initial estimation methods, types 1 and 2, for mixtures M1 and M2 at some specified

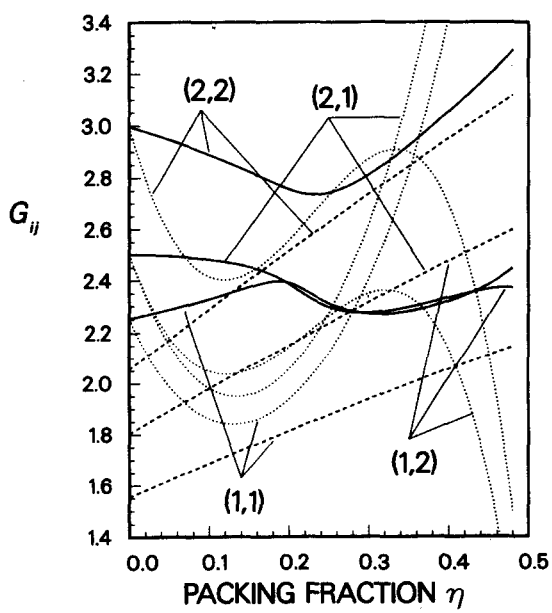

FIG. 4. Comparison between initial estimates and solution values for the $\{G_{ij}\}$ for mixture M1 at $x_1 = 0.65$ and temperature $T^* = 0.717$. The solid lines represent the solution values, the dashed lines result from the type 1 estimate, and the dotted lines from type 2.

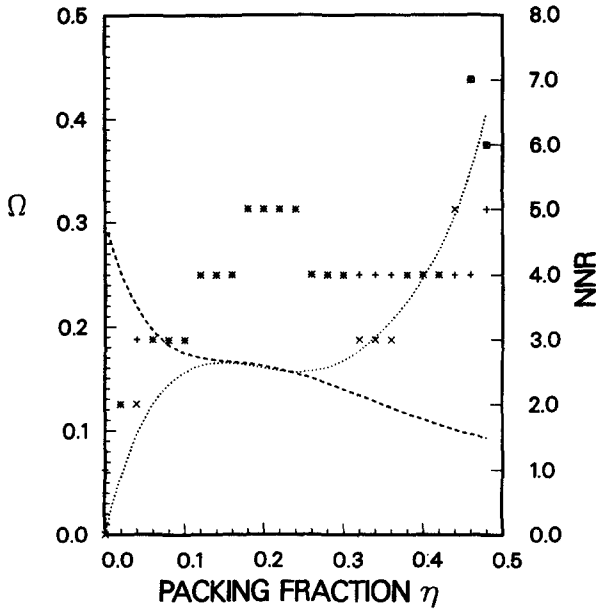

FIG. 5. Errors arising from the initial estimates for mixture M1 at $x_1 = 0.65$ and fixed temperature $T^* = 0.717$. The lines (dashed for type 1, dotted for type 2) give the error Ω [see Eq. (15)], to the left, for the initial estimates. The discrete markers (+ for type 1, × for type 2) represent the number of Newton–Raphson iterations NNR, to the right, needed to obtain an error $\Omega < 10^{-6}$. The circles surrounding the last two × signs indicate that for those conditions the type 2 estimate led to unphysical solutions.

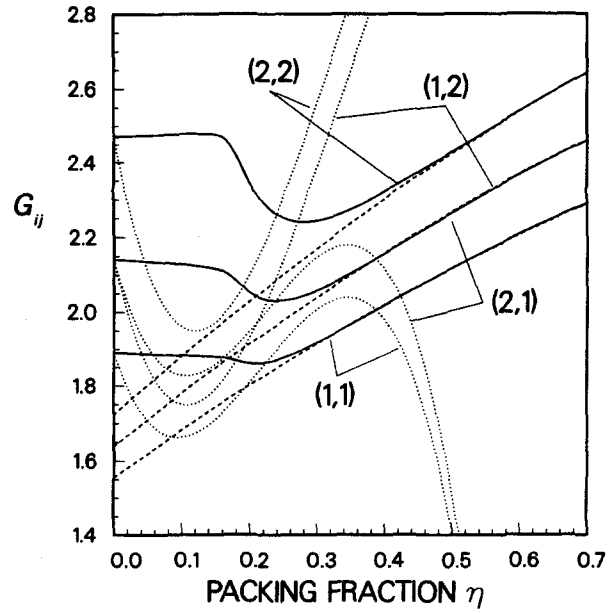

FIG. 7. Same as Fig. 4 for mixture M2 at $x_1 = 0.25$ and temperature $T^* = 1.495$.

composition and temperature. In Figs. 3–5 (for M1), η has been extended to reach the region of liquid–liquid separation (see Fig. 1). The type 2 estimation becomes unreliable at high densities (see the growing deviation from the solution values of the type 2 estimates for G_{ij} in Figs. 4 and 7). It led to unphysical solutions for the last two points in Fig. 5. At liquid-like densities, which is the range of interest in MSA applications, the type 1 estimate produces very good results.

This is especially true for the close-to-ideal M2 mixture. The number of iterations to convergence (in Figs. 5 and 8) is greater near the peak of the vapor–liquid region, that is, in the neighborhood of the critical point. In that area, when the density is varied at constant temperature, the D_{ij} (in Figs. 3 and 6) go through a maximum, while the G_{ij} (in Figs. 4 and 7) display an inflexion point. Observe also in Figs. 3 and 6 (in this figure examine the high density limit) the similar variation of D_{11} and D_{21} on the one hand, and D_{12} and D_{22} on the other. In Sec. VI and, especially, Appendix D, we will come back to this topic.

One obvious strategy would be to try both estimates and use the one giving a smaller error Ω. Furthermore, a few direct substitution steps, say four, according to Eqs. (20)

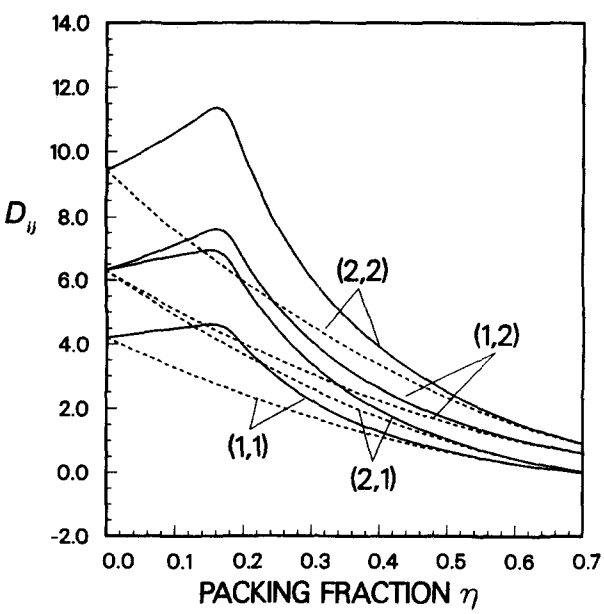

FIG. 6. Same as Fig. 3 for mixture M2 at $x_1 = 0.25$ and temperature $T^* = 1.495$.

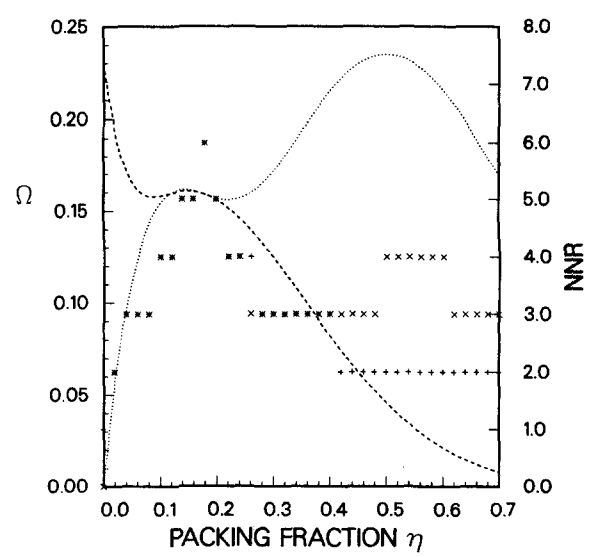

FIG. 8. Same as Fig. 5 for mixture M2 at $x_1 = 0.25$ and temperature $T^* = 1.495$.

TABLE II. Solutions for the system of nonlinear equations.

Mixture	x_1	η	$kT/\lvert\epsilon_{11}\rvert$	G_{11}	G_{12}	G_{22}	D_{11}	D_{12}	D_{21}	D_{22}
M1	0.35	0.30	0.900	2.1809	2.3763	2.8094	5.8193	3.5966	5.4083	5.1626
		0.30	0.717	2.2666	2.3985	2.8290	7.7763	4.8521	7.3235	6.8838
		0.46	0.900	2.3394	2.5769	3.1261	4.7473	1.4419	3.9992	2.4856
		0.46	0.717	2.4034	2.5686	3.1290	6.1989	1.8537	5.2405	3.1738
M1	0.50	0.30	0.900	2.1639	2.3403	2.7974	5.8322	3.1717	5.4262	4.8194
		0.30	0.717	2.2621	2.3530	2.8135	8.0154	4.3573	7.5443	6.4727
		0.46	0.900	2.3181	2.5276	3.1259	4.6911	0.7518	3.9532	1.9724
		0.46	0.717	2.3947	2.5019	3.1365	6.3110	0.9157	5.3172	2.4680
M1	0.65	0.30	0.900	2.1377	2.2881	2.7951	5.8484	2.5040	5.4574	4.2796
		0.30	0.717	2.2713	2.2753	2.8119	8.6585	3.5544	8.1535	5.8077
		0.46	0.900	2.2835	2.4557	3.1607	4.5839	−0.3633	3.8736	1.1452
		0.46	0.717	2.4025	2.3707	3.2236	6.7710	−0.9081	5.6640	1.0978
		0.46	0.717	2.6999[a]	2.1475[a]	3.3906[a]	9.6649[a]	−2.4399[a]	7.8804[a]	−0.0785[a]
M2	0.25	0.30	1.450	1.9166	2.0582	2.2480	2.3442	4.2767	3.5328	6.3766
		0.30	1.200	1.9180	2.0684	2.3052	3.3915	6.3435	5.1029	9.4599
		0.46	1.450	2.0783	2.2209	2.3846	0.9267	2.0942	1.4162	3.1177
		0.46	1.200	2.0783	2.2200	2.3869	1.1438	2.6021	1.7471	3.8740
M2	0.50	0.30	1.450	1.9152	2.0602	2.2512	2.3327	4.1976	3.5116	6.2536
		0.30	1.200	1.9180	2.0720	2.2963	3.1551	5.7540	4.7455	8.5748
		0.46	1.450	2.0684	2.2125	2.3782	1.0031	2.1814	1.5240	3.2398
		0.46	1.200	2.0683	2.2121	2.3817	1.2375	2.7048	1.8794	4.0174
M2	0.75	0.30	1.450	1.9139	2.0624	2.2549	2.3204	4.1142	3.4884	6.1234
		0.30	1.200	1.9182	2.0759	2.2951	3.0235	5.4031	4.5438	8.0448
		0.46	1.450	2.0570	2.2030	2.3711	1.0915	2.2795	1.6484	3.3763
		0.46	1.200	2.0569	2.2034	2.3763	1.3437	2.8161	2.0288	4.1718

[a] This is an unphysical solution.

and (21) are sure to yield a significantly improved estimate. In general, however, this will not translate into appreciable computer time reductions. We have carried out most of our work employing the type 1, infinite temperature guess, Eqs. (16) and (17), with very satisfactory results. The amount of computer time usually required varied between 3 and 5 s (in double precision) in a HP-9000.

Table II presents the solution values G_{ij}, with $G_{12} = G_{21}$, and D_{ij} for Eqs. (12) and (13) for mixtures M1 and M2 at different compositions, packing fractions (or densities), and temperatures. Other conditions kept constant, a decrease in temperature produces higher D_{ij}, which can be expected from Eqs. (4), (5), (6), and (8) for $r \geqslant \sigma_{ij}$. The G_{ij} experience, in general, the same variation. At lower temperatures, the interaction potential acts more effectively which, given our Yukawa attraction, results in higher RDF values near contact (see Table III). Thus, see Eq. (14), the G_{ij} variables increase.

At liquid-like densities, when the fluid becomes denser (all other conditions fixed) the G_{ij} augment, due to higher RDF near contact, and the D_{ij} diminish. Observe, however, that the behavior of these variables is different at vapor-like densities (Figs. 3, 4, 6, and 7).

B. Criteria for physical solutions

The system of nonlinear equations represented by Eqs. (12) and (13) has multiple solutions. Of them, only those for which all eight variables take real values should concern us. Among these real solutions (if they exist) only one will be physical. Therefore, once a real solution is obtained, we must ascertain whether it is physical. To that effect, the only probably failure-proof method consists in monitoring the smooth variation of the solution variables, (G_{ij},D_{ij}) when the thermodynamic conditions are gradually changed, beginning at some point yielding a known, physical solution. There are four possible, independent starting points (all other conditions kept constant): $T=\infty$ (Giunta *et al.*[12]), $z=\infty$, $\rho=0$, and $x_2=0$ (Cummings and Smith[11]). (The last two are rather troublesome since the system may traverse a region of phase separation when increasing ρ or x_2, and therefore the procedure would break down.) For all cases investigated, the solution obtained by using the initial estimation given by Eqs. (16) and (17), type 1, and the Newton–Raphson method met the above physicality criterion.

There are of course weaker conditions that any physical solution must satisfy. For example, Cummings and Smith control the physical validity of their solutions through the test of

$$G_{12} = G_{21}\,, \tag{22}$$

and Giunta *et al.* use the more demanding requirement of equality between the contact values of the crossed RDF [see Eq. (31)],

$$g_{12}(\sigma_{12}) = g_{21}(\sigma_{21})\,. \tag{23}$$

Moreover, Eq. (14) can give reasonable limits for all G_{ij} when $g_{ij}(r)$ is substituted by some mean effective value, say more than 1 and less than 5 (a higher superior limit may be needed if z is large, see Sec. V).

Working with purposefully chosen bad initial estimates,

TABLE III. MSA radial distribution function contact values.

Mixture	x_1	η	$kT/\lvert\epsilon_{11}\rvert$	$g_{11}(\sigma_{11})$	$g_{12}(\sigma_{12})$	$g_{22}(\sigma_{22})$
M1	0.35	0.30	0.900	2.7388	2.4878	2.6629
		0.30	0.717	2.9456	2.5794	2.7411
		0.46	0.900	4.0196	3.9456	4.4544
		0.46	0.717	4.1618	3.9656	4.4738
M1	0.50	0.30	0.900	2.7353	2.4736	2.6787
		0.30	0.717	2.9511	2.5544	2.7479
		0.46	0.900	4.0498	3.9748	4.5587
		0.46	0.717	4.1944	3.9754	4.5770
M1	0.65	0.30	0.900	2.7299	2.4542	2.7100
		0.30	0.717	2.9764	2.5169	2.7670
		0.46	0.900	4.0908	4.0194	4.7306
		0.46	0.717	4.2564	3.9766	4.7638
		0.46	0.717	4.4386[a]	3.8922[a]	4.7977[a]
M2	0.25	0.30	1.450	2.3742	2.5331	2.7622
		0.30	1.200	2.4185	2.6165	2.9160
		0.46	1.450	3.9635	4.1573	4.4046
		0.46	1.200	3.9689	4.1702	4.4317
M2	0.50	0.30	1.450	2.4088	2.5700	2.7999
		0.30	1.200	2.4499	2.6431	2.9280
		0.46	1.450	4.0415	4.2430	4.4992
		0.46	1.200	4.0483	4.2578	4.5287
M2	0.75	0.30	1.450	2.4515	2.6157	2.8470
		0.30	1.200	2.4915	2.6839	2.9619
		0.46	1.450	4.1395	4.3505	4.6176
		0.46	1.200	4.1479	4.3674	4.6498

[a]This is an unphysical solution.

we have been able to obtain a limited number of unphysical solutions, although only at high density plus low temperature. (With our algorithm those estimates normally result in either the physical solution or no convergence.) In all cases, these solutions satisfied the conditions given by Eqs. (22) and (23) and all G_{ij} had physically reasonable values (see Table II where we include an example). Furthermore, all thermodynamic properties acquired similar values (see Tables III and IV) to the ones calculated from the physical solution reached with our usual procedure (type 1 estimate). Only when the radial distribution functions were computed did the nonphysical nature of all such solutions become apparent (see Fig. 11).

IV. CALCULATION OF MSA THERMODYNAMIC PROPERTIES

In this section we follow again Blum and Høye's work, developing their expressions to their final, ready-to-use form. Once the variables $\{D_{ij}\},\{G_{ij}\}$ have been found, we first determine the remaining factor correlation function parameters, i.e., $\{a_{ij}\}$, $\{b_{ij}\}$, and $\{C_{ij}\}$:

$$C_{ij} = -\sum_l (\delta_{il} - \frac{2\pi}{z^2}\rho_l G_{il} e^{-z\sigma_l}) D_{lj} , \tag{24}$$

where δ_{il} is Kronecker's delta. It is convenient to define

$$f_{ij} = (C_{ij} + D_{ij}) e^{z\sigma_i} = \frac{2\pi}{z^2} \sum_l \rho_l G_{il} D_{lj} . \tag{25}$$

We also need the following two quantities, already utilized in Blum and Høye's paper:

$$M_j = -\frac{1}{z^2} \sum_m \rho_m M_m^{(a)} D_{mj} - \frac{2\pi}{z^4} \sum_{mk} \rho_k \rho_m (1 - M_m^{(a)} e^{-z\sigma_m}) G_{mk} D_{kj} , \tag{26}$$

$$N_j = \frac{1}{z^3} \sum_m \rho_m L_{mj}^{(a)} D_{mj} + \frac{2\pi}{z^5} \sum_{mk} \rho_k \rho_m (1 + z\lambda_{jm} - L_{mj}^{(a)} e^{-z\sigma_m}) G_{mk} D_{kj} , \tag{27}$$

where all coefficients whose superscript is between parenthesis or is equal to zero (below) are defined in Appendix B. The parameters $\{a_{ij}\}$ and $\{b_{ij}\}$ are given by

$$A_j = A_j^0 (1 + M_j) - \frac{4}{\sigma_j^2} B_j^0 N_j , \tag{28}$$

$$a_{ij} = A_j , \tag{29}$$

$$b_{ij} = b_{ij}^0 (1 + M_j) + A_i^0 N_j . \tag{30}$$

The radial distribution functions contact values, $g_{ij}(\sigma_{ij})$, are equal to the sudden change or "jump" in $h_{ij}(r)$ at $r = \sigma_{ij}$. From Eq. (7), it is evident that this is produced by a discontinuity of $Q'_{ij}(r)$ at contact. Therefore,

$$g_{ij}(\sigma_{ij}) = \frac{1}{2\pi\sigma_{ij}} (b_{ij} - C_{ij}) , \tag{31}$$

while the MSA, or PY, hard-sphere contact values are

$$g_{ij}^0(\sigma_{ij}) = \frac{b_{ij}^0}{2\pi\sigma_{ij}} . \tag{32}$$

Table III presents the MSA contact values resulting from the solutions listed in Table II. As expected at liquid-like densities, an increase in density leads to higher contact values. The same effect is produced by a decrease in temperature. The exception to this last rule, for M1 at $x_1 = 0.65$, $\eta = 0.46$, arises because that system is about to undergo a liquid–liquid separation at the lower temperature (see Fig. 1). Therefore, as each component tends to segregate into different phases, the contact value of the crossed RDF decreases. This anomalous variation of $g_{12}(\sigma_{12})$ with temperature can be used as an early indication of liquid–liquid transition.

The configurational energy U^c per molecule is equal to

$$\frac{U^c}{N} = -\frac{2\pi}{z}\rho \sum_{ij} x_i x_j \epsilon_{ij}\sigma_{ij} G_{ij} , \tag{33}$$

N being the total number of molecules in the system, and $\{x_i\}$ representing the mole fractions. Normally, all energies are scaled by kT but in this case we prefer not to do so because at infinite temperature, even if the mixture behaves as a hard-sphere one for all practical purposes, the configurational energy is nonzero.

The inverse isothermal compressibility calculated through the fluctuation theorem is given by

$$\chi^{-1} = \frac{1}{kT}\left(\frac{\partial P}{\partial \rho}\right)_T = \sum_j x_j \left(\frac{A_j}{2\pi}\right)^2 . \tag{34}$$

For the corresponding hard-sphere mixture we have

$$\chi_0^{-1} = \sum_j x_j \left(\frac{A_j^0}{2\pi}\right)^2 . \tag{35}$$

Within the MSA, it is possible to obtain closed form expressions for both the virial pressure P^V (the one which is calculated directly) and the energy pressure P^E. Unfortunately, the same is not true for the compressibility pressure. The incremental[17] values of the first two are

$$\frac{\Delta P^V}{\rho kT} = \frac{2\pi}{3}\rho \sum_{ij} x_i x_j \sigma_{ij}^3 [\, g_{ij}(\sigma_{ij}) - g_{ij}^0(\sigma_{ij})\,] + J , \tag{36}$$

$$\frac{\Delta P^E}{\rho kT} = \frac{\pi}{3}\rho \sum_{ij} x_i x_j \sigma_{ij}^3 \{[\, g_{ij}(\sigma_{ij})\,]^2 - [g_{ij}^0(\sigma_{ij})\,]^2\} + J , \tag{37}$$

where

$$J = \frac{2\pi}{3}\rho \sum_{ij} x_i x_j K_{ij}\left(G'_{ij} - \frac{1}{z} G_{ij}\right), \tag{38}$$

and the symbol G'_{ij} represents

$$G'_{ij} = z\left(\frac{\partial \hat{g}_{ij}(s)}{\partial s}\right)_{s=z} e^{z\sigma_{ij}} = -z\int_{\sigma_{ij}}^{\infty} r^2 e^{-z(r-\sigma_{ij})} g_{ij}(r)dr . \tag{39}$$

The computation of these derivatives is presented in Appendix C. Within the MSA the properties calculated from the energy equation are more accurate than those obtained from the (virial) pressure or the isothermal compressibility equations.[18] Therefore, P^E should be preferred over P^V.

The incremental Helmholtz free energy is given by

$$\frac{\Delta A}{NkT} = \frac{U^c}{NkT} - \frac{\Delta P^E}{\rho kT} + \tfrac{1}{2}(\chi^{-1} - \chi_0^{-1}) . \tag{40}$$

Lastly, the incremental chemical potentials $\Delta\mu_i$, calculated from the energy equation, can be obtained from

$$\frac{\Delta\mu_i}{kT} = -\frac{2\pi}{z}\sum_j \rho_j K_{ij} G_{ij} - \frac{1}{2}\sum_j \rho_j [\,\tilde{c}_{ij}(0) - \tilde{c}_{ij}^0(0)\,] , \tag{41}$$

where $\tilde{c}_{ij}(0)$ are the three-dimensional Fourier transforms of the direct correlation functions, while $\tilde{c}_{ij}^0(0)$ correspond to the hard-sphere case:

$$\tilde{c}_{ij}(0) = 4\pi\int_0^{\infty} r^2 c_{ij}(r)dr . \tag{42}$$

The difference between these two values, needed in Eq. (41), is given by

$$\tilde{c}_{ij}(0) - \tilde{c}_{ij}^0(0) = (\overline{Q}_{ij} - \overline{Q}_{ij}^0) + (\overline{Q}_{ji} - \overline{Q}_{ji}^0) - \sum_l \rho_l (\overline{Q}_{il}\overline{Q}_{jl} - \overline{Q}_{il}^0\overline{Q}_{jl}^0) , \tag{43}$$

where

$$\overline{Q}_{ij} = \int_{\lambda_{ji}}^{\infty} Q_{ij}(r)dr , \tag{44}$$

and therefore,

$$\overline{Q}_{ij} = \tfrac{1}{6}a_{ij}\sigma_i^3 - \tfrac{1}{2}b_{ij}\sigma_i^2 - (1/z^2)C_{ij}M_i^{(a)} + (1/z^2)f_{ij} , \tag{45}$$

$$\overline{Q}_{ij}^0 = \tfrac{1}{6}a_{ij}^0\sigma_i^3 - \tfrac{1}{2}b_{ij}^0\sigma_i^2 . \tag{46}$$

The equations above have been written so that numerical troubles are avoided should any ρ_i approach zero.

Table IV gives results for the thermodynamic properties. We used the Carnahan–Mansoori–Starling–Leland (CMSL)[19] equation of state to calculate the hard-sphere contributions (except for P^V, for which we used the hard-sphere MSA or PY value). For the Helmholtz free energy and the chemical potentials we give the density residual quantities, i.e., for any thermodynamic property X:

$$X^r(\rho,T,x_i) = X(\rho,T,x_i) - X^*(\rho,T,x_i) , \tag{47}$$

$X^*(\rho,T,x_i)$ being the corresponding perfect gas mixture quantity.

The balance between (interaction) potential and (temperature-determined) kinetic energy helps explain the variation of the thermodynamic properties. At higher density the molecules get closer together, at distances of lower energy and, for our Yukawa potential, greater attraction. A decrease in temperature reduces the kinetic energy of the molecules, making them more influenceable by the interaction potential. This accounts for the changes in the configurational energy (note the sign).

The values for P^V are systematically lower than those of P^E. This is a typical trait of the MSA (for it underestimates the direct correlations). The variation of both compressibility factors is consistent with the behavior of real fluids.

TABLE IV. Thermodynamic properties.

Mixture	x_1	η	$\frac{kT}{\lvert\epsilon_{11}\rvert}$	$-\frac{U^c}{N\lvert\epsilon_{11}\rvert}$	χ^{-1}	$\frac{P^V}{\rho kT}$	$\frac{P^E}{\rho kT}$	$-\frac{A^r}{NkT}$	$\frac{\mu_1^r}{kT}$	$\frac{\mu_2^r}{kT}$
M1	0.35	0.30	0.900	2.3200	4.0986	0.1618	0.7765	0.7347	−1.2910	−0.7789
		0.30	0.717	2.3450	2.6718	−0.7536	0.0032	1.3960	−2.3382	−2.3784
		0.46	0.900	3.9086	29.3834	2.1994	3.8467	0.4172	−0.0835	3.7827
		0.46	0.717	3.9155	26.5542	0.6300	2.4235	1.5266	−1.8792	0.8532
M1	0.50	0.30	0.900	2.4277	3.7467	0.0363	0.6287	0.8731	−1.6206	−0.8683
		0.30	0.717	2.4609	2.2917	−0.9081	−0.1407	1.5659	−2.8092	−2.6041
		0.46	0.900	4.0632	28.3340	1.9799	3.5591	0.6429	−0.3955	4.2279
		0.46	0.717	4.0770	25.4476	0.3766	2.0985	1.7970	−2.4261	1.0290
M1	0.65	0.30	0.900	2.6283	3.2931	−0.1820	0.4045	1.0938	−2.0644	−0.9926
		0.30	0.717	2.6866	1.8145	−1.2031	−0.4090	1.8462	−3.4466	−2.8999
		0.46	0.900	4.3621	27.3885	1.6443	3.1833	0.9881	−0.7881	4.8785
		0.46	0.717	4.3990	24.3786	−0.0680	1.6314	2.2295	−3.1498	1.2834
		0.46	0.717	4.4856[a]	24.4891[a]	−0.2287[a]	1.5617[a]	2.2254[a]	−3.2498[a]	1.2818[a]
M2	0.25	0.30	1.450	5.7006	1.8986	−1.2028	−0.4538	1.9832	−1.7877	−3.9869
		0.30	1.200	5.8085	0.4351	−2.2841	−1.2694	2.8085	−2.8977	−5.8045
		0.46	1.450	9.3230	27.2329	0.2626	2.0519	2.3207	0.4186	−1.8312
		0.46	1.200	9.3281	23.9875	−1.4958	0.4253	3.6605	−1.6143	−5.1089
M2	0.50	0.30	1.450	5.0752	2.7490	−0.6367	−0.0009	1.5774	−1.5284	−3.6280
		0.30	1.200	5.1289	1.2947	−1.5760	−0.7694	2.3100	−2.6711	−5.4878
		0.46	1.450	8.3117	28.8412	1.2280	2.9183	1.6402	1.2259	−0.6696
		0.46	1.200	8.3156	25.9641	−0.3227	1.4768	2.8347	−0.7904	−3.9254
M2	0.75	0.30	1.450	4.4504	3.6776	−0.0529	0.4760	1.1599	−1.1919	−3.1601
		0.30	1.200	4.4777	2.3294	−0.8614	−0.2190	1.8012	−2.3479	−5.0372
		0.46	1.450	7.2940	30.7384	2.2426	3.8423	0.9332	2.2679	0.8327
		0.46	1.200	7.2965	28.2307	0.9007	2.5865	1.9814	0.2720	−2.3956

[a] This is an unphysical solution.

For our Yukawa model fluid under some conditions, the intermolecular attractions bringing the molecules together prevail over their kinetic energy. As a result, an external force, a negative pressure, is necessary to take the molecules apart from one another, so that they will occupy the full volume specified by the density. This explains the appearance of negative compressibility factors in Table IV. The region of negative pressures is probably "metastable," in the sense that two-phase calculations are likely to show the oc-

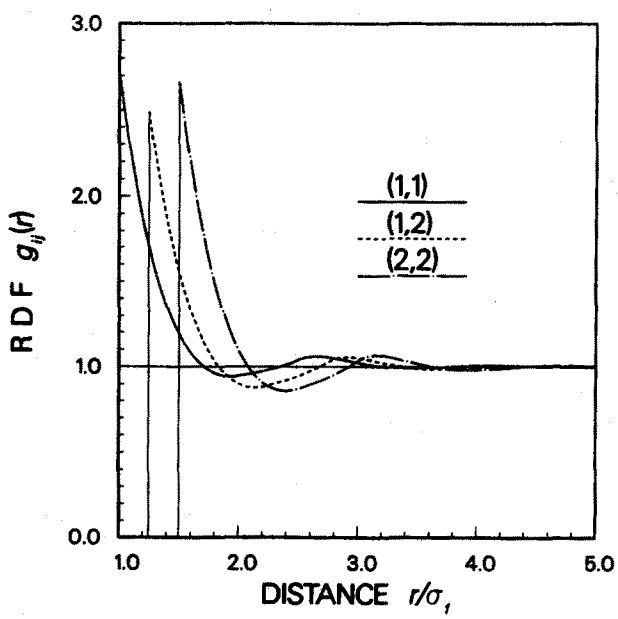

FIG. 9. Radial distribution functions $g_{ij}(r)$ for mixture M1 at $x_1 = 0.35$, $\eta = 0.30$, and $T^* = 0.900$.

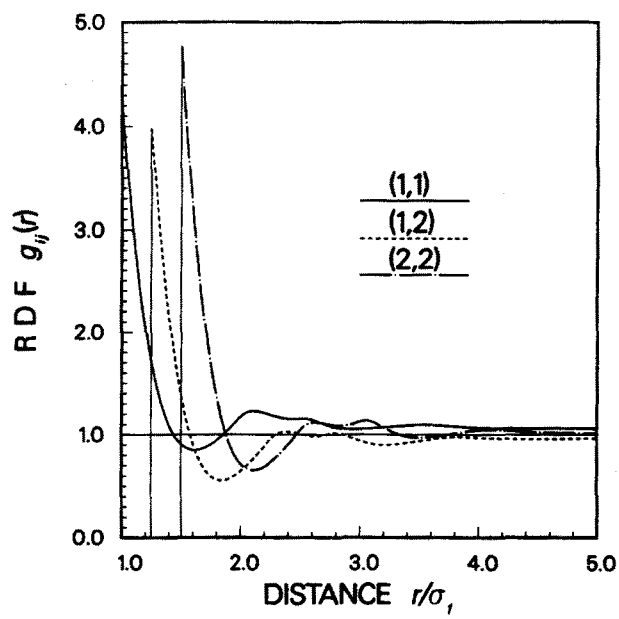

FIG. 10. Radial distribution functions $g_{ij}(r)$ for mixture M1 at $x_1 = 0.65$, $\eta = 0.46$, and $T^* = 0.717$. This somewhat slow convergence to 1 arises because these conditions are very close to liquid–liquid separation, see Fig. 1.

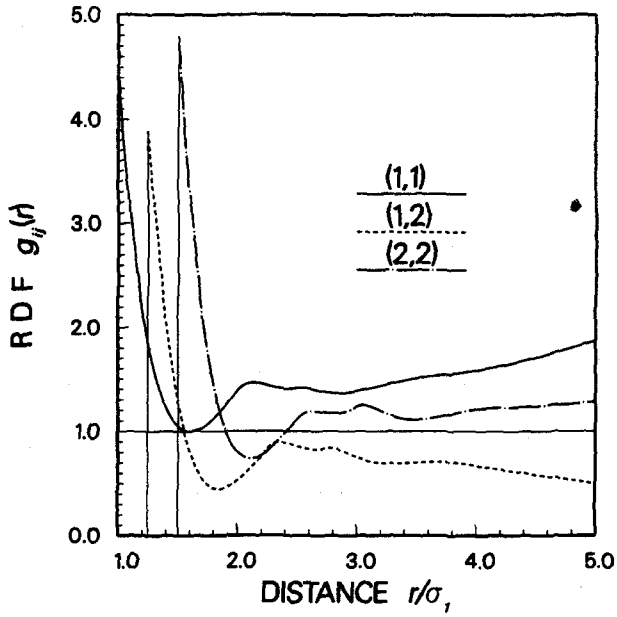

FIG. 11. Radial distribution functions $g_{ij}(r)$ for mixture M1 at $x_1 = 0.65$, $\eta = 0.46$, and $T^* = 0.717$. These divergent RDF's result from the unphysical solution in Table II.

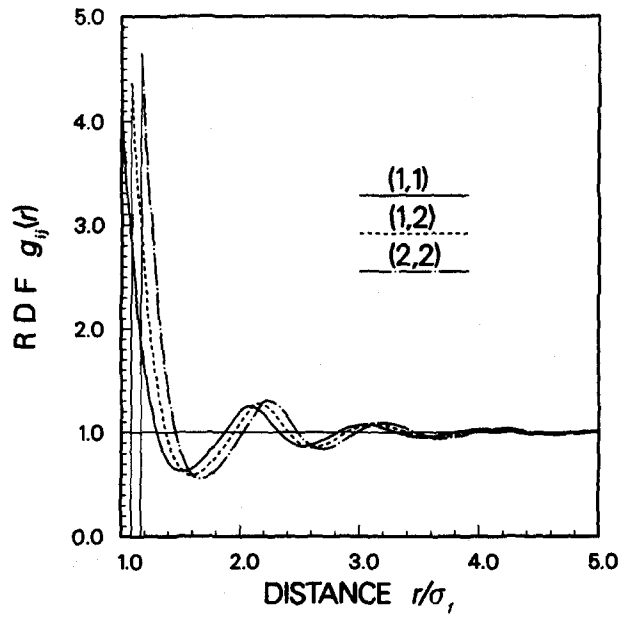

FIG. 13. Radial distribution functions $g_{ij}(r)$ for mixture M2 at $x_1 = 0.75$, $\eta = 0.46$, and $T^* = 1.200$.

currence of a phase transition before reaching those conditions.

For a more realistic model fluid, the introduction of three-body corrections would increase the pressure. (The mutual attraction between two real molecules at a given distance diminishes if a third one approaches them.)

Within a homogeneous phase, the chemical potentials usually increase with both higher density and temperature (keeping constant the other independent variables in the set ρ, T, x_i). Table IV reflects this physical behavior. Moreover, it is interesting to compare results for the two components. The variation (at constant ρ and x_i) of μ_i^r/kT with temperature can be shown to be directly related to the soft part of the interaction potential. Therefore, that variation should be greater for the component subject to a larger (in absolute value) global potential energy, i.e., $4\pi \Sigma_j x_j \int r^2 \phi_{ij}(r) dr$, where the integral is performed from σ_{ij} to ∞. Again, the results in Table IV agree with this qualitative indication. In mixture M1, whose second component is clearly larger, an increase in density produces a much more marked increment in μ_2^r.

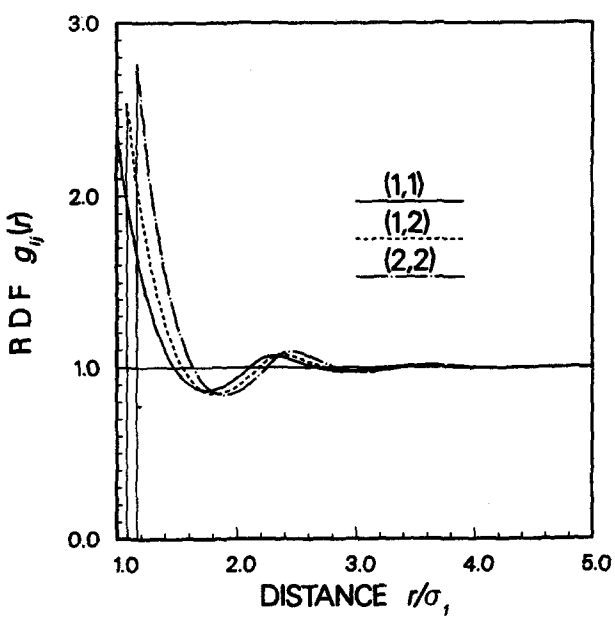

FIG. 12. Radial distribution functions $g_{ij}(r)$ for mixture M2 at $x_1 = 0.25$, $\eta = 0.30$, and $T^* = 1.450$.

Figures 9 to 13 present the pair radial distribution functions obtained through a modification of Perram's algorithm[20] for hard spheres. It can be see that the combination of higher density and lower temperature (compare Figs. 9 and 10 for mixture M1, and Figs. 12 and 13 for M2) produces larger and longer-ranged fluctuations in the RDF. That is, the fluid becomes more "structured." Figure 11 makes evident that the solution originating it (see Table II) is unphysical. Observe the notable similarity, disregarding the divergence, between the physical RDF (Fig. 10) and their unphysical counterparts.

V. LARGE Z APPROXIMATION

In this section we examine the dependency of the solution to the Blum and Høye[5] equations on the Yukawa exponent z, particularly at large values of z, adequate for GMSA applications. Throughout this Section, all $\{K_{ij}\}$ are assumed positive, which in the MSA means attractive interactions.

Suppose that $\{\rho_i\}$, $\{\sigma_i\}$, and $\{K_{ij}\}$ have been fixed. Taking the limit $z \to \infty$ in the expressions for the coefficients in Appendix B and using them in Eqs. (12) and (13), the solution is immediately given by

$$D_{ij} = 2\pi K_{ij} , \tag{48}$$

$$G_{ij} = \frac{b_{ij}^0}{2\pi} + \frac{K_{ij}}{2} . \tag{49}$$

It is possible to obtain Eq. (48) directly from Eq. (6) for $r \geqslant \sigma_{ij}$. Using Eq. (4) for the left-hand side and Eq. (8) for the right-hand side, one gets

$$2\pi K_{ij} = D_{ij} - \sum_l \rho_l D_{il} \int_{\lambda_{ij}}^{\infty} Q_{jl}(t) e^{-z(t-\lambda_{ij})} dt , \quad (50)$$

and in the limit $z \to \infty$, Eq. (48) is recovered.

From Eqs. (24), (26), (27), (30), and (31), the limiting RDF contact values are given by

$$g_{ij}(\sigma_{ij}) = \frac{b_{ij}^0}{2\pi\sigma_{ij}} + \frac{K_{ij}}{\sigma_{ij}}$$
$$= g_{ij}^0(\sigma_{ij}) + \frac{\epsilon_{ij}}{kT} , \quad (51)$$

where $g_{ij}^0(\sigma_{ij})$ are the PY contact values for the hard-sphere mixture, and ϵ_{ij} are the MSA interaction potential parameters. Actually, when the limit $z \to \infty$ is taken, the MSA radial distribution functions for that extreme case of the Yukawa potential will be exactly equal to their hard-sphere counterparts, except at contact.

For a given set of positive $\{K_{ij}\}$, Eq. (51) represents the maximum possible contact values attainable by varying z. This point will be proven analytically for large values of z, using an asymptotic approximate solution, and numerically for the full range of z values.

For large values of z, one can expect to obtain a very good approximation by including only terms in z^0 and z^{-1}. Here we solve the complete problem neglecting all terms of higher order in z^{-1} and exponential $e^{-z\sigma_i}$ terms. As a result, Eq. (12) becomes

$$\sum_l \left(\frac{1}{z} C_{lj}^{(z)} + \delta_{lj} \right) D_{il} = 2\pi K_{ij} , \quad (52)$$

where

$$C_{lj}^{(z)} = \frac{\pi}{1-\eta_3} \rho_l \sigma_l \sigma_j . \quad (53)$$

By solving the linear system given by Eq. (52) we obtain the approximate $\{D_{ij}\}$ solution. Taking derivatives with respect to z we get,

$$\frac{1}{z} \sum_l C_{lj}^{(z)} D'_{il} + D'_{ij} = \frac{1}{z^2} \sum_l C_{lj}^{(z)} D_{il} . \quad (54)$$

Neglecting smaller terms and realizing that all $C_{lj}^{(z)}$ are positive and that so are the $\{D_{ij}\}$ at large values of z, Eq. (48), we can assure that

$$D'_{ij} > 0 \quad \text{for all } i,j . \quad (55)$$

Within our approximation, Eqs. (24), (26), (27), (30), and (31), remembering, Eq. (49), that the $\{G_{ij}\}$ remain finite, result in

$$g_{ij}(\sigma_{ij}) = \frac{b_{ij}^0}{2\pi\sigma_{ij}} + \frac{1}{2\pi\sigma_{ij}} \left(D_{ij} - \frac{1}{z} \sum_m C_{mi}^{(z)} D_{mj} \right)$$
$$= g_{ij}^0(\sigma_{ij}) + \frac{K_{ij}}{\sigma_{ij}} - \frac{1}{2\pi\sigma_{ij}} \frac{1}{z}$$
$$\times \left(\sum_m C_{mi}^{(z)} D_{mj} + \sum_l C_{lj}^{(z)} D_{il} \right) . \quad (56)$$

Taking derivatives with respect to z,

$$g'_{ij}(\sigma_{ij}) = \frac{\partial}{\partial z} [\, g_{ij}(\sigma_{ij}) \,] = \frac{1}{2\pi\sigma_{ij}}$$
$$\times \left(D'_{ij} - \frac{1}{z} \sum_m C_{mi}^{(z)} D'_{mj} + \frac{1}{z^2} \sum_m C_{mi}^{(z)} D_{mj} \right) , \quad (57)$$

and neglecting smaller terms we obtain,

$$g'_{ij}(\sigma_{ij}) = \frac{1}{2\pi\sigma_{ij}} \left(D'_{ij} + \frac{1}{z^2} \sum_m C_{mi}^{(z)} D_{mj} \right) . \quad (58)$$

From Eqs. (48), (53), and (55), for positive $\{K_{ij}\}$ and at large values of z, we find that

$$g'_{ij}(\sigma_{ij}) > 0 \quad \text{for all } i,j . \quad (59)$$

Consequently, when z decreases so do the RDF contact values. This result complements the investigation on the influence of z by Giunta *et al.*[12]

Physically, an increase in z shortens the range of the attractive interaction potential. This means that at large values of z, a given molecule attracts any other coming close to contact without having to compete with nearby molecules, and therefore the RDF contact values become high. This notion of "competition" is further illustrated by the fact that at zero density, when (on average) there are no nearby molecules and thus no such competition, the contact values are independent of z. Making the appropriate substitutions at $\rho = 0$, for any z, Eq. (51) is recovered, with the hard-sphere contribution $g_{ij}^0(\sigma_{ij}) = 1$,

$$g_{ij}(\sigma_{ij}) = 1 + \frac{\epsilon_{ij}}{kT} . \quad (60)$$

This can be derived, Eqs. (1), (2), (4), and (5), from the MSA version of the exact theoretical result, at $\rho = 0$,

$$g_{ij}(r) = e^{-\phi_{ij}(r)/kT} . \quad (61)$$

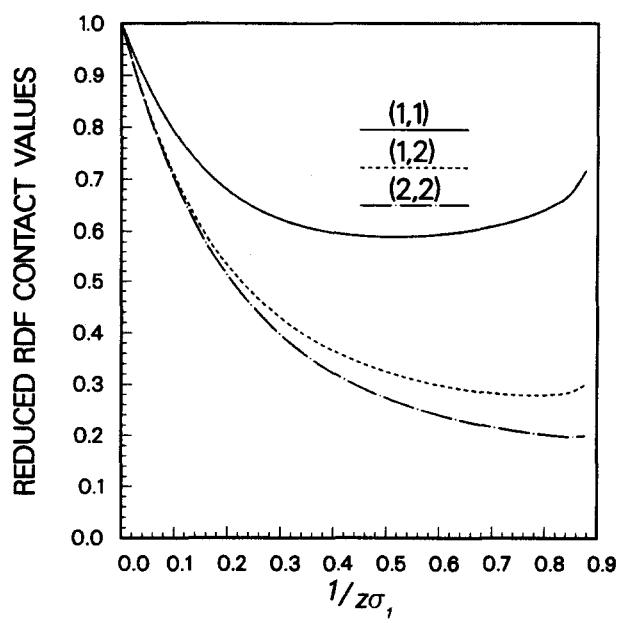

FIG. 14. Reduced RDF contact values, defined as $[g_{ij}(\sigma_{ij}) - g_{ij}^0(\sigma_{ij})] \times kT/\epsilon_{ij}$, as functions of the Yukawa exponent z for mixture M1 at $x_1 = 0.35$, $\eta = 0.30$, and $T^* = 0.900$.

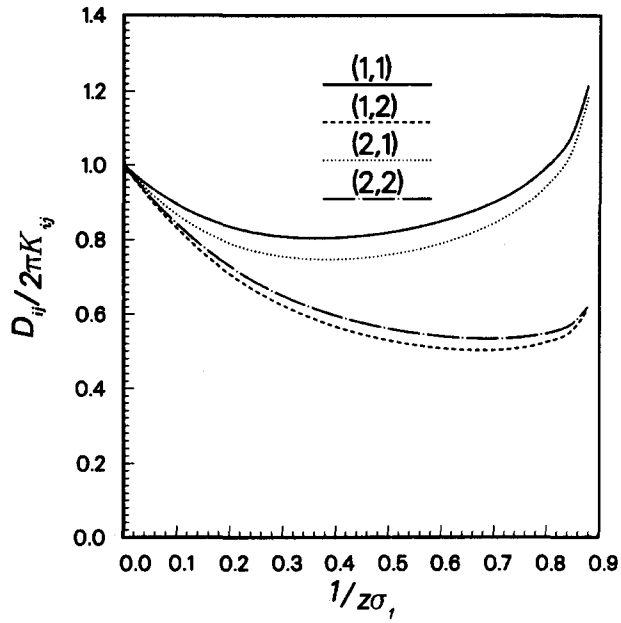

FIG. 15. Values of $D_{ij}/(2\pi K_{ij})$ as functions of the Yukawa exponent z. Same mixture and conditions as for Fig. 14.

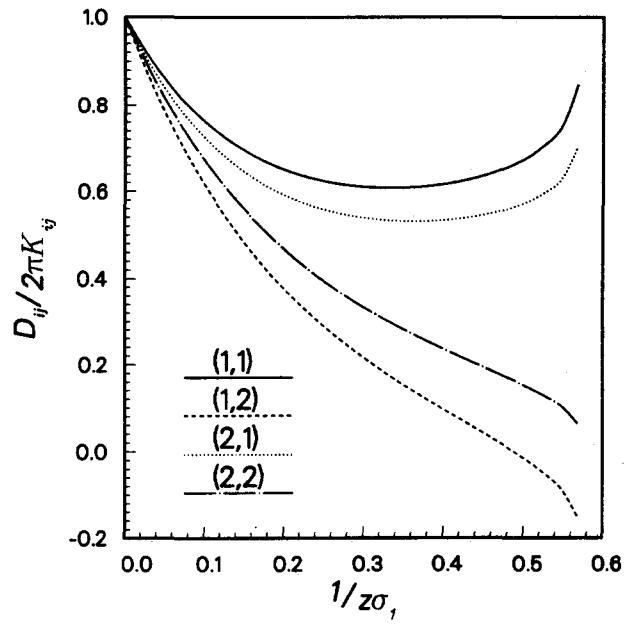

FIG. 17. Values of $D_{ij}/(2\pi K_{ij})$ as functions of the Yukawa exponent z. Same mixture and conditions as for Fig. 16.

Equations (52)–(59) constitute a very good approximation at large values of z and allow an analytical study of the problem. For smaller values of z, however, one must solve the full system of nonlinear equations. The results thus obtained are represented in Figs. 14 to 21 for several specific cases. These figures show the z dependency of the RDF contact values, normalized according to $[g_{ij}(\sigma_{ij}) - g^0_{ij}(\sigma_{ij})] \times kT/\epsilon_{ij}$ [see Eq. (51)], and D_{ij}, expressed as $D_{ij}/(2\pi K_{ij})$. As was expected, the variation with z from the infinite limit values was more marked, for both kinds of variables, at higher densities. It is interesting to observe the very similar values for D_{11} and D_{21} on the one hand and D_{12} and D_{22} on the other when such scaling factors are used. Note that our initial estimates [see Eq. (17) and Appendix B] produce the same pairing. This very important parallelism is analyzed in detail in Appendix D, where we prove that when $K_{12} = \sqrt{K_{11}K_{22}}$ the following pairing results: $D_{11}/K_{11} = D_{21}/K_{21}$ and $D_{12}/K_{12} = D_{22}/K_{22}$. In all cases, z was lowered until the solution procedure did no longer find real solutions for Eqs. (12) and (13). Obviously, a decrease in z increases the range of the interactions, leading to greater global intermolecular attraction and a more pronounced imbalance (if there is any)

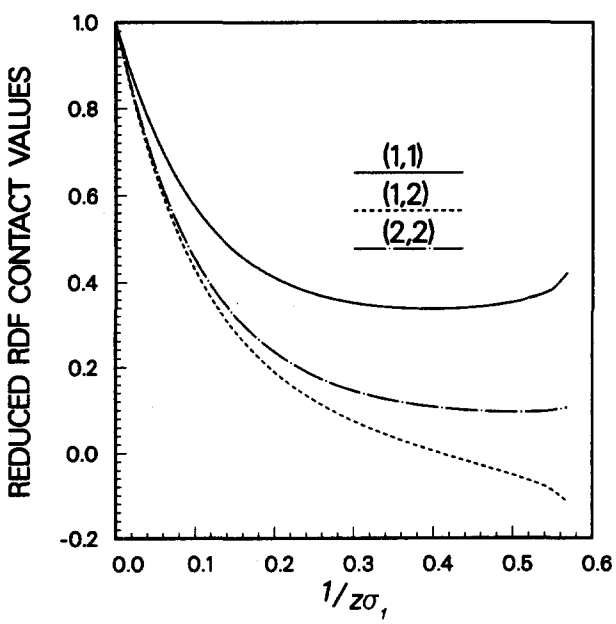

FIG. 16. Same as Fig. 14 for mixture M1 at $x_1 = 0.65$, $\eta = 0.46$, and $T^* = 0.717$.

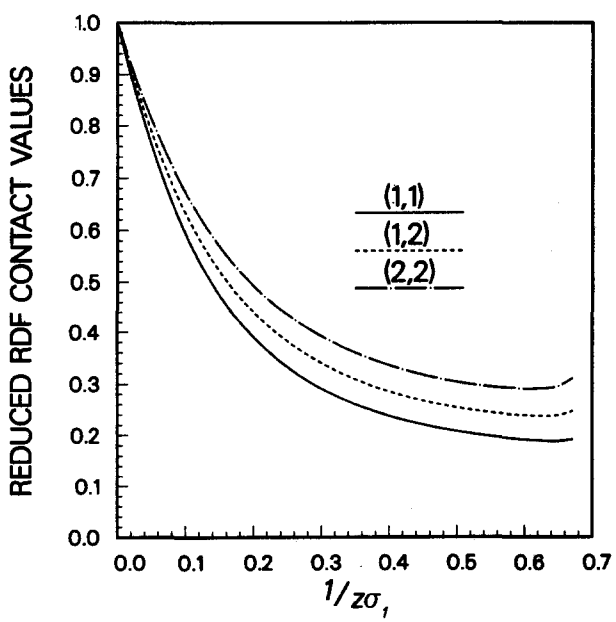

FIG. 18. Same as Fig. 14 for mixture M2 at $x_1 = 0.25$, $\eta = 0.30$, and $T^* = 1.450$.

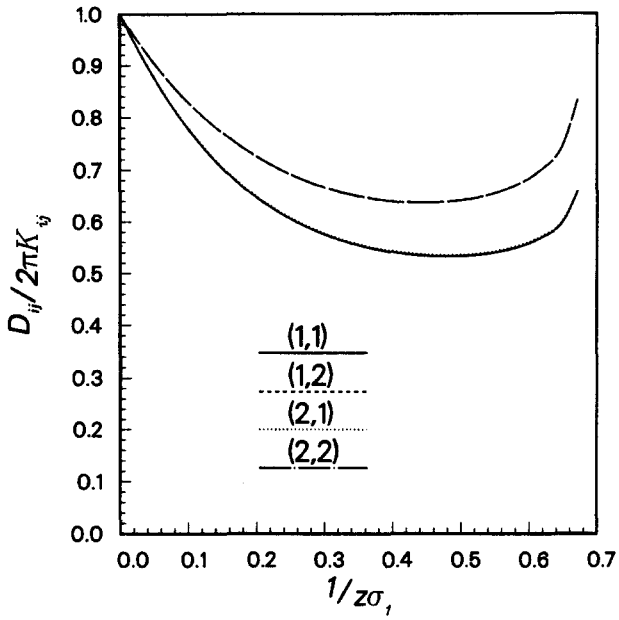

FIG. 19. Values of $D_{ij}/(2\pi K_{ij})$ as functions of the Yukawa exponent z. Same mixture and conditions as for Fig. 18. The curves for D_{11} and D_{21} (below) are practically coincident, and so are those for D_{12} and D_{22} too.

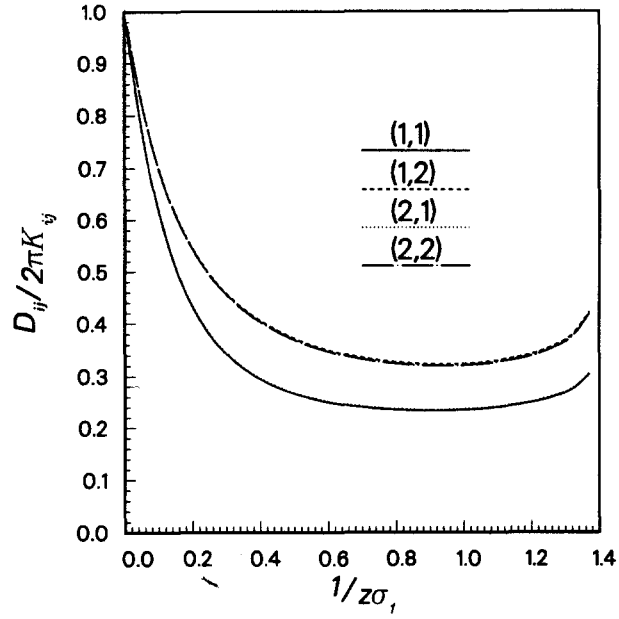

FIG. 21. Values of $D_{ij}/(2\pi K_{ij})$ as functions of the Yukawa exponent z. Same mixture and conditions as for Fig. 20. The curves for D_{11} and D_{21} (below) are practically coincident, and the same is also true for D_{12} and D_{22}.

between like- and unlike-particle interactions. As a result, both vapor–liquid and liquid–liquid separation regions, in Figs. 1 and 2, are displaced to higher temperatures. It is also worth noting that in Fig. 16, where the results end at liquid–liquid separation (see Fig. 1), the normalized contact value for $g_{12}(r)$ is smaller than either of those for $g_{11}(r)$ or $g_{22}(r)$ along the whole range of z.

For subsequent discussion, we give the approximate expression for Eq. (28) at large values of z:

$$A_j = A_j^0 - \frac{1}{z}\frac{2\pi}{(1-\eta_3)}\sum_m \rho_m \sigma_m D_{mj} \,. \tag{62}$$

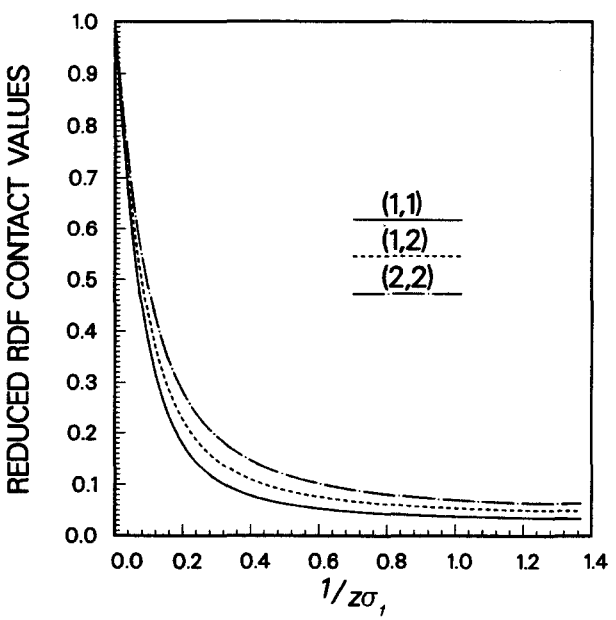

FIG. 20. Same as Fig. 14 for mixture M2 at $x_1 = 0.75$, $\eta = 0.46$, and $T^* = 1.200$.

These coefficients are needed in the calculation of the inverse isothermal compressibility, Eq. (34).

We will use the above conclusions to examine the results by Giunta *et al.*[12] Following the GMSA approach, these authors study hard-sphere mixtures. They vary $\{K_{ij}\}$ and z so that the MSA results fit the isothermal compressibility and the RDF contact values derived from the CMSL[19] equation of state. They present numerical results (the required $\{K_{ij}\}$ and z) for three different hard-sphere mixtures (all at a packing fraction $\eta = 0.49$, and a composition $x_1 = x_2 = 0.5$) characterized by the diameter ratios σ_1/σ_2: 0.9, 0.3, 0.5. Table V collects their results for the above parameters. However, none of them are dimensionless. The K_{ij} have dimensions of length, Eq. (5), and z of reciprocal length, Eq. (1). Therefore, for the values in Table V to have a concrete meaning they must be given units or, more conveniently, these parameters must be scaled (the K_{ij} divided, z multiplied) by some specific length. The obvious choice is to use either σ_1 or σ_2.

In Tables VI, for the RDF contact values, and VII, for the isothermal compressibility, we compare the CMSL results with those obtained from the MSA (MSA_{ex}) when using the parameters in Table V if we consider them scaled

TABLE V. GMSA parameters for the Yukawa direct correlation functions used by Giunta *et al.* in reproducing the CMSL hard-sphere results.

Mixture designation[a]	σ_1/σ_2	K_{11}	K_{12}	K_{22}	z
G1	0.90	1.179	1.360	1.582	28.851
G2	0.30	0.047	0.257	1.492	30.095
G3	0.50	0.222	0.584	1.649	28.770

[a] All mixtures studied at a packing fraction $\eta = 0.49$ and for a composition $x_1 = x_2 = \frac{1}{2}$.

TABLE VI. Comparison of RDF contact values $g_{ij}(\sigma_{ij})$ for the mixtures investigated by Giunta *et al.*

			Parameters $\{K_{ij}\}$ and z scaled by σ_1		σ_2	
Mixture[a]	(i,j)	CMSL	MSA_{ex}	MSA_{ap}	MSA_{ex}	MSA_{ap}
G1	(1,1)	5.427	5.434	5.422	5.490	5.472
	(1,2)	5.653	5.655	5.642	5.716	5.697
	(2,2)	5.911	5.913	5.900	5.983	5.964
G2	(1,1)	2.952	2.899	2.899	2.947	2.939
	(1,2)	3.562	3.446	3.446	3.581	3.568
	(2,2)	5.979	5.358	5.358	5.980	5.964
G3	(1,1)	3.810	3.699	3.698	3.792	3.779
	(1,2)	4.551	4.357	4.355	4.530	4.513
	(2,2)	6.218	5.771	5.769	6.201	6.181

[a] All mixtures studied at a packing fraction $\eta = 0.49$ and for a composition $x_1 = x_2 = \frac{1}{2}$.

by σ_1 and σ_2. Apparently, Giunta *et al.* employed σ_1 scaling for their $\sigma_1/\sigma_2 = 0.9$ mixture and σ_2 scaling for the other two.

Tables VI and VII also include the approximate MSA results (MSA_{ap}) calculated through our large z approximation: Equations (52) and (56) for the RDF contact values and Eqs. (52), (62), and (34) for the inverse isothermal compressibility. It can be seen that the agreement between the exact and approximate MSA results is quite good, especially when the parameters in Table V are taken as scaled by the smaller σ_1, since that leads to a higher effective value for z. Therefore, our approximate equations can provide a good starting point ($\{K_{ij}\},z$) for the GMSA description of hard-sphere mixtures according to the scheme by Giunta *et al.*

We close this section with one final word regarding the thermodynamic properties in the limit $z \to \infty$. In that case, the Yukawa potential becomes a hard-sphere one with a finite surface adhesivity. This leads to the corresponding hard-sphere RDFs', but for a finite "jump" at contact. This finite discontinuity does not affect the thermodynamic properties, though, as can be seen taking the limit in the expressions of Sec. IV. Only the virial pressure, as given by Eq. (36), is an exception, for the delta function integration is not valid in the presence of a doubly discontinuous RDF at contact.

TABLE VII. Comparison of inverse isothermal compressibility χ^{-1} values for the mixtures investigated by Giunta *et al.*

		Parameters $\{K_{ij}\}$ and z scaled by σ_1		σ_2	
Mixture[a]	CMSL	MSA_{ex}	MSA_{ap}	MSA_{ex}	MSA_{ap}
G1	51.511	51.899	51.474	50.784	50.220
G2	34.997	38.327	38.318	34.989	34.695
G3	42.250	45.473	45.410	41.908	41.463

[a] All mixtures studied at a packing fraction $\eta = 0.49$ and for a composition $x_1 = x_2 = \frac{1}{2}$.

VI. MIXTURES OF EQUAL-SIZED COMPONENTS

This section is concerned with binary mixtures where both (spherical) components have the same diameter. In Sec. VI A, we show that for an equimolar, symmetric mixture Baxter's equations can be decoupled. Section VI B evaluates two recent approximations for equal-sized Yukawa mixtures due to Jedrzejek, Konior, and Streszewski (JKS).[15] We compare, for several mixtures, results obtained according to their method with our exact MSA results.

A. Baxter's factorized form of the Ornstein–Zernike equation. Decoupling for an equal-sized, symmetric, equimolar mixture

For equal-sized, symmetric mixture we understand a binary mixture in which both components have equal diameters $\sigma_1 = \sigma_2$ and both kinds of like-particle interaction are identical [$\phi_{11}(r) = \phi_{22}(r)$ for all r]. Actually, the only difference with respect to a pure substance is that the crossed interactions are different from the like-particle ones:

$$\phi_{11}(r) = \phi_{22}(r) \neq \phi_{12}(r) = \phi_{21}(r) . \tag{63}$$

In this section we show that for this special mixture, when the two components are present in equal concentrations $\rho_1 = \rho_2 = \frac{1}{2}\rho$, Baxter's factorized version of the Ornstein–Zernike equation for mixtures can be decoupled into two parts, each describing an hypothetical pure component. No presumptions regarding the interaction potential or approximations (such as the MSA) are introduced in the process. This does not include the assumption that the direct correlation functions have a finite range, since otherwise Baxter's form is not strictly valid.

Equations (6) and (7) give Baxter's version of the Ornstein–Zernike equation. In this case (equal diameters), all integrals are to be performed from zero to infinity. From symmetry considerations, it is clear that

$$h_{11}(r) = h_{22}(r) \neq h_{12}(r) = h_{21}(r) . \tag{64}$$

Taking this into account, we add first and then subtract the versions of Eq. (7) for h_{11} and h_{21} to get the following two equations (+ and − , respectively):

$$\begin{aligned} 2\pi r[h_{11}(r) \pm h_{21}(r)] = & -[Q'_{11}(r) \pm Q'_{21}(r)] \\ & + \pi\rho \int (r-t)[h_{11}(|r-t|) \\ & \pm h_{21}(|r-t|)] \\ & \times [Q_{11}(t) \pm Q_{21}(t)]\,dt . \end{aligned} \tag{65}$$

Doing the same with the expressions for h_{22} and h_{12} we arrive at

$$\begin{aligned} 2\pi r[h_{22}(r) \pm h_{12}(r)] = & -[Q'_{22}(r) \pm Q'_{12}(r)] \\ & + \pi\rho \int (r-t)[h_{22}(|r-t|) \\ & \pm h_{12}(|r-t|)] \\ & \times [Q_{22}(t) \pm Q_{12}(t)]\,dt . \end{aligned} \tag{66}$$

From Eqs. (64), (65), and (66), we can assure that

$$Q_{11}(r) \pm Q_{21}(r) = Q_{22}(r) \pm Q_{12}(r) , \tag{67}$$

and therefore,

$$Q_{11}(r) = Q_{22}(r)\,, \tag{68}$$

$$Q_{12}(r) = Q_{21}(r)\,. \tag{69}$$

Taking these last results to Eq. (6) we can verify by simple substitution that the expressions for $c_{11}(r)$ and $c_{22}(r)$ are completely equivalent and so are those for the pair $c_{12}(r), c_{21}(r)$. Therefore,

$$c_{11}(r) = c_{22}(r) \neq c_{12}(r) = c_{21}(r)\,. \tag{70}$$

Observe that Eq. (70) has been *proved*, not *assumed*. This result can also be reached by directly applying the method used above to the Ornstein–Zernike equation for mixtures. In that case it is not precise to assume that the direct correlation functions are finitely ranged.

If we define the following two (+ and −) generic correlation functions:

$$\alpha_{\pm}(r) = \tfrac{1}{2}[\alpha_{11}(r) \pm \alpha_{12}(r)]\,, \tag{71}$$

where α can be h, c, or Q, we can write Eq. (65) as

$$2\pi r h_{\pm}(r) = -Q'_{\pm}(r) + 2\pi\rho \times \int (r-t)h_{\pm}(|r-t|)Q_{\pm}(t)dt\,. \tag{72}$$

Adding $c_{11}(r)$ and $c_{12}(r)$ given by Eq. (6), and then substracting them, the result is

$$\begin{aligned} 2\pi r[c_{11}(r) \pm c_{12}(r)] &= -[Q'_{11}(r) \pm Q'_{12}(r)] \\ &\quad + \frac{1}{2}\rho \int \{[Q_{11}(t)Q'_{11}(r+t) \\ &\quad + Q_{12}(t)Q'_{12}(r+t)] \\ &\quad \pm [Q_{21}(t)Q'_{11}(r+t) + Q_{22}(t)Q'_{12}(r+t)]\}dt \end{aligned} \tag{73}$$

which in view of Eqs. (68), (69), and (71) leads to

$$2\pi r c_{\pm}(r) = -Q'_{\pm}(r) + \rho \int Q_{\pm}(t)Q'_{\pm}(r+t)dt\,. \tag{74}$$

It is obvious that Eqs. (74) and (72) describe two different (+ and −) pure components.

TABLE VIII. Interaction potential parameters for the equal-sized mixtures of Tables IX and X.

Mixture designation	ϵ_{11}[a]	ϵ_{12}	ϵ_{22}	$z\sigma_1$
E1	1.000	0.818 18	1.000	1.800
E2	1.000	0.900 00	1.150	1.600

[a] All ϵ_{ij} scaled by $|\epsilon_{11}|$.

B. Evaluation of the JKS approximations for equal-sized Yukawa mixtures

In a recent publication,[15] JKS propose two approximate solution methods for equal-sized binary Yukawa mixtures. Their first method, which we term approx. 1, was developed for symmetric mixtures, i.e., $K_{11} = K_{22}$. The second, approx. 2 here, was designed for asymmetric mixtures, $K_{11} \neq K_{22}$, and was based on the mapping of these mixtures into an equimolar, symmetric one, solving it according to approx. 1 and mapping the results back to the asymmetric case. Both methods are based on the assumption that the number density and concentration fluctuations are uncorrelated $[S_{NC}(0) = 0]$. Thus JKS are able to decouple the mixture into two hypothetical pure components which can be solved by the usual methods[21] for pure Yukawa fluids.

For a given set of $\{K_{ij}\}$ coefficients, the assumption $S_{NC}(0) = 0$ is correct only at the specific composition $\{x_i\}$ that satisfies

$$x_1K_{11} + (x_2 - x_1)K_{12} - x_2K_{22} = 0\,. \tag{75}$$

In that case, both JKS methods yield the exact MSA solution. For a symmetric mixture the composition required by Eq. (75) is $x_1 = x_2 = \frac{1}{2}$. For an asymmetric mixture, Eq. (75) can only be satisfied by a physical set of $\{x_i\}$ values if K_{12} lies outside the range (K_{11}, K_{22}).

Table VIII gives the characteristics of the two mixtures used in our comparison between the JKS approximations and our exact MSA results. Mixture E1 was already used by JKS in their work, although the parameters were given in a different form. We compare values for the configurational

TABLE IX. Comparison, for the symmetric mixture E1, between the JKS approximation 1 and the exact MSA results for some thermodynamic properties.

x_1	η	$\frac{kT}{\lvert\epsilon_{11}\rvert}$	$-\frac{(U^c)_{ex}}{N\lvert\epsilon_{11}\rvert}$	$-\frac{(U^c)_{apl}}{N\lvert\epsilon_{11}\rvert}$	$(\chi^{-1})_{ex}$	$(\chi^{-1})_{apl}$	$\frac{(P^V)_{ex}}{\rho kT}$	$\frac{(P^V)_{apl}}{\rho kT}$
0.200	0.375	0.936	4.6603	4.6590	8.5652	8.5604	−0.6645	−0.6625
	0.375	0.700	4.6783	4.6751	4.8014	4.7865	−2.7711	−2.7693
	0.492	0.936	6.4052	6.4046	42.7746	42.7720	1.9128	1.9123
	0.492	0.700	6.4114	6.4103	37.2934	37.2874	−0.9902	−0.9889
0.400	0.375	0.936	4.5227	4.5224	8.9112	8.9103	−0.4818	−0.4800
	0.375	0.700	4.5433	4.5426	5.2466	5.2436	−2.5349	−2.5322
	0.492	0.936	6.2201	6.2200	43.2756	43.2751	2.1615	2.1576
	0.492	0.700	6.2426	6.2421	37.9601	37.9585	−0.6894	−0.6928
0.500	0.375	0.936	4.5057	4.5057	8.9541	8.9541	−0.4594	−0.4579
	0.375	0.700	4.5269	4.5269	5.3009	5.3009	−2.5065	−2.5048
	0.492	0.936	6.1977	6.1977	43.3379	43.3379	2.1915	2.1937
	0.492	0.700	6.2341	6.2341	38.0424	38.0424	−0.6785	−0.6744

TABLE X. Comparison, for the asymmetric mixture E2, between the two JKS approximations and the exact MSA results for some thermodynamic properties.

x_1	η	$\frac{kT}{\lvert\epsilon_{11}\rvert}$	$-\frac{(U^c)_{ex}}{N\lvert\epsilon_{11}\rvert}$	$-\frac{(U^c)_{ap1}}{N\lvert\epsilon_{11}\rvert}$	$-\frac{(U^c)_{ap2}}{N\lvert\epsilon_{11}\rvert}$	$(\chi^{-1})_{ex}$	$(\chi^{-1})_{ap1}$	$(\chi^{-1})_{ap2}$	$\frac{(P^V)_{ex}}{\rho kT}$	$\frac{(P^V)_{ap1}}{\rho kT}$	$\frac{(P^V)_{ap2}}{\rho kT}$
0.150	0.340	1.300	5.4611	5.4577	5.1219	5.4629	5.4569	6.0467	−0.4072	−0.4062	−0.0978
	0.340	0.900	5.5029	5.4897	5.1613	1.4891	1.4430	2.2539	−2.6657	−2.6599	−2.2329
	0.500	1.300	8.4776	8.4761	7.9657	48.8071	48.8039	49.7724	3.0973	3.0997	3.5737
	0.500	0.900	8.4821	8.4804	[a]	42.0761	42.0678	[a]	−0.4178	−0.4187	[a]
0.300	0.340	1.300	5.2041	5.2010	5.0610	5.9010	5.8950	6.1429	−0.1706	−0.1699	−0.0409
	0.340	0.900	5.2422	5.2310	5.0946	2.0835	2.0440	2.3875	−2.3269	−2.3198	−2.1430
	0.500	1.300	8.0825	8.0815	7.8686	49.5269	49.5236	49.9301	3.4661	3.4646	3.6658
	0.500	0.900	8.0940	8.0915	[a]	43.1152	43.1056	[a]	0.1057	0.0976	[a]
0.500	0.340	1.300	4.9818	4.9807	4.9807	6.2734	6.2716	6.2716	0.0334	0.0318	0.0318
	0.340	0.900	5.0125	5.0091	5.0091	2.5771	2.5661	2.5661	−2.0315	−2.0270	−2.0270
	0.500	1.300	7.7431	7.7427	7.7427	50.1413	50.1403	50.1403	3.7826	3.7808	3.7808
	0.500	0.900	7.7638	7.7624	7.7624	43.9986	43.9947	43.9947	0.5491	0.5460	0.5460
0.714 286	0.340	1.300	4.8958	4.8958	4.8958	6.4092	6.4092	6.4092	0.1117	0.1113	0.1113
	0.340	0.900	4.9202	4.9202	4.9202	2.7582	2.7582	2.7582	−1.9130	−1.9155	−1.9155
	0.500	1.300	7.6106	7.6106	7.6106	50.3655	50.3655	50.3655	3.9054	3.9017	3.9017
	0.500	0.900	7.6196	7.6196	7.6196	44.3195	44.3195	44.3195	0.7426	0.7406	0.7406
0.850	0.340	1.300	4.9249	4.9247	4.9037	6.3543	6.3539	6.4966	0.0847	0.0819	0.1610
	0.340	0.900	4.9476	4.9491	4.8650	2.6826	2.6811	2.8802	−1.9494	−1.9516	−1.8456
	0.500	1.300	7.6547	7.6551	7.5280	50.2753	50.2752	50.5081	3.8636	3.8635	3.9837
	0.500	0.900	7.6582	7.6581	7.5340	44.1897	44.1892	44.5252	0.6896	0.6902	0.8553

[a] Absence of real solution.

energy, inverse isothermal compressibility, and direct virial compressibility factor [Eq. (36) plus the PY hard-sphere contribution].

Table IX evaluates approx. 1 for the symmetric mixture E1. As expected, this method produces exact results at $x_1 = 0.5$. (The agreement for the virial pressure is not perfect because the required derivatives have been calculated numerically in the approximate procedure.) Surprisingly, approx. 1 maintains an excellent accuracy for other compositions. In Table X, we apply approximately 1 and 2 to the asymmetric mixture E2.[22] Both methods yield exact results when Eq. (75) is satisfied ($x_1 = 0.714\,286$). Again, approx. 1 (which treats the mixture as though it were symmetric) gives very good results, in fact much better than the asymmetric method approx. 2. The latter even fails to obtain real solutions under some conditions.

VII. CONCLUSIONS

We have presented a complete, efficient numerical algorithm for solving the Blum and Høye[5] MSA equations for binary mixtures. Its application to multicomponent mixtures is straightforward. This algorithm is much faster than the existing ones[11,12] and is reliable in that it converges to the physical solution, if it exists. We analyze the cases in which no (real) solutions can be found and show that the present method is able to detect not only vapor–liquid transitions but also liquid–liquid separations. Analytic expressions are given for the calculation of all MSA thermodynamic properties. For high values of z, we have developed an accurate linear approximation which can be used advantageously in the GMSA study of hard-sphere mixtures. Earlier results[12] in this field have also been clarified.

For equimolar, equal-sized, symmetric mixtures we have shown that the Baxter[6] factorized version of the Ornstein–Zernike equation for mixtures can be completely decoupled. Also for equal-sized mixtures, we have evaluated two recent approximations[15] finding one of them to be surprisingly accurate.

Our algorithm is directly applicable to the study of liquid metals[14] where—since it is not restricted to equal-size components or absence of correlation between the number density and the concentration fluctuations—it should represent an important advance over the previous methods. Another very promising application, made possible by this algorithm, is the use of Yukawa mixtures as a reference fluid in perturbation theories for mixtures. Pure Yukawa fluids have already been successfully utilized[23] in this fashion.

This work will soon be complemented with an evaluation of the MSA results produced here by comparison with the corresponding Monte Carlo values. Also in progress is the use of the present algorithm in the determination of phase diagrams for binary mixtures.

The knowledge acquired here as to the numerical solution of the simplest case (one-Yukawa potential) of the BH equations[5] will be of great importance for the solution of mixtures with more realistic potentials obtained by linear combination of Yukawa tails.

ACKNOWLEDGMENTS

We thank J. Konior for useful discussions and help in numerical calculations. B. E. Gammon also contributed many valuable comments. This work was supported by GRI Contract No. 5086-260-1240. E. Arrieta gladly acknowledges the support of the Industrial Engineering School of Bilbao (Spain) and, in particular, of J. A. Legarreta.

APPENDIX A

The following is a list of typographical errors in Blum and Høye's paper,[5] on which the present work is based. (1) Equation (8): a minus sign (−) must precede $Q'_{ij}(r)$. (2) Equation (29): an $e^{z\sigma_{ij}}$ factor should multiply the coefficient K_{ij}. (3) Equation (34): the $e^{-z\sigma_{ij}}$ factor outside the braces on the right-hand side must be divided by z^2. (4) Equation (35): the last z must be dividing, not multiplying. (5) Equation (36): the last term within the braces should have a z^2 divisor, instead of just z. (6) Equation (37): the factor preceding the braces must be $e^{-z\lambda_{ji}}$ instead of $e^{-z\lambda_{ij}}$. (7) Equation (43): it must be substituted by our Eq. (37). (8) Equation (44): a ρ divisor is missing on the right-hand side.

APPENDIX B

Expressions for the coefficients appearing in Eqs. (12) and (13) are given here. We recall that the quantities $\{\rho_i\}$, $\{\sigma_i\}$, $\{K_{ij}\}$, and z constitute the data of the problem. The symbol $\{\delta_{ij}\}$ represents Kronecker's delta. We define the following parameters corresponding to the hard-sphere case:

$$A_j^0 = \frac{2\pi}{(1-\xi_3)^2}(1-\xi_3+3\sigma_j\xi_2)\,, \tag{B1}$$

$$B_j^0 = \frac{2\pi}{(1-\xi_3)^2}\left(-\frac{3}{2}\sigma_j^2\xi_2\right), \tag{B2}$$

$$b_{ij}^0 = \frac{2\pi}{(1-\xi_3)^2}\left[\frac{3}{2}\sigma_i\sigma_j\xi_2+\sigma_{ij}(1-\xi_3)\right], \tag{B3}$$

where

$$\xi_\nu = \frac{\pi}{6}\sum_i \rho_i\sigma_i^\nu\,. \tag{B4}$$

Obviously, ξ_3 is equal to the packing fraction η. We also need the functions

$$\vartheta_1(x) = 1-x-e^{-x}, \tag{B5}$$

$$\vartheta_2(x) = 1-x+\tfrac{1}{2}x^2-e^{-x}, \tag{B6}$$

and the coefficients

$$M_m^{(a)} = 1+z\sigma_m\,, \tag{B7}$$

$$L_{mj}^{(a)} = 1+z\sigma_{mj}+\tfrac{1}{2}z^2\sigma_m\sigma_j\,, \tag{B8}$$

$$H_{ij}^a = zb_{ij}^0\vartheta_1(z\sigma_l)+A_j^0\vartheta_2(z\sigma_l)\,, \tag{B9}$$

$$G_{lj}^{(a)} = zA_l^0\vartheta_1(z\sigma_l)-\frac{4}{\sigma_j^2}B_j^0\vartheta_2(z\sigma_l)\,, \tag{B10}$$

$$F_{mlj}^{(a)} = L_{mj}^{(a)}G_{lj}^{(a)}-zM_m^{(a)}H_{lj}^{(a)}\,, \tag{B11}$$

$$E_{mlj}^{(a)} = (1+z\lambda_{jm})G_{lj}^{(a)}-zH_{lj}^{(a)}\,, \tag{B12}$$

$$D_{mjl}^{(a)} = \frac{1}{z^6}\left[\rho_m F_{mjl}^{(a)}+\delta_{mj}z^4(1-\tfrac{1}{2}e^{-z\sigma_j})\right], \tag{B13}$$

$$C_{kmjl}^{(a)} = \frac{2\pi}{z^8}\rho_k\left[\rho_m(E_{mjl}^{(a)}-F_{mjl}^{(a)}e^{-z\sigma_m}) + \tfrac{1}{2}\delta_{mj}z^4(1-e^{-z\sigma_j})^2\right], \tag{B14}$$

$$A_{ij}^{(4)} = 2\pi K_{ij}\,, \tag{B15}$$

$$A_{lj}^{(3)} = \frac{1}{z^3}\rho_l H_{jl}^{(a)}-\delta_{lj}\,, \tag{B16}$$

$$A_{mjl}^{(2)} = \rho_l D_{mjl}^{(a)}\,, \tag{B17}$$

$$A_{kmjl}^{(1)} = \rho_l C_{kmjl}^{(a)}\,, \tag{B18}$$

$$H_{ij}^{(b)} = zb_{ij}^0+A_j^0\,, \tag{B19}$$

$$G_{ij}^{(b)} = zA_i^0-\frac{4}{\sigma_j^2}B_j^0\,, \tag{B20}$$

$$F_{mij}^{(b)} = L_{mj}^{(a)}G_{ij}^{(b)}-zM_m^{(a)}H_{ij}^{(b)}\,, \tag{B21}$$

$$E_{mij}^{(b)} = (1+z\lambda_{jm})G_{ij}^{(b)}-zH_{ij}^{(b)}\,, \tag{B22}$$

$$D_{mlj}^{(b)} = 2\pi\rho_l D_{mlj}^{(a)}\,, \tag{B23}$$

$$C_{mkij}^{(b)} = \frac{2\pi}{z^6}\rho_m\left[\rho_k(E_{kij}^{(b)}-F_{kij}^{(b)}e^{-z\sigma_k}) - \tfrac{1}{2}\delta_{ik}z^4e^{-z\sigma_i}\right], \tag{B24}$$

$$B_{ij}^{(5)} = \frac{1}{z}A_j^0+b_{ij}^0\,, \tag{B25}$$

$$B_{lj}^{(4)} = \frac{2\pi}{z^3}\rho_l H_{lj}^{(a)}-2\pi\delta_{lj}\,, \tag{B26}$$

$$B_{mij}^{(3)} = \frac{1}{z^4}\rho_m F_{mij}^{(b)}+\tfrac{1}{2}\delta_{im}\,, \tag{B27}$$

$$B_{kmlij}^{(2)} = \delta_{ik}D_{mlj}^{(b)}+\delta_{lm}C_{mkij}^{(b)}\,, \tag{B28}$$

$$B_{klmj}^{(1)} = 2\pi\rho_l C_{kmlj}^{(a)}\,. \tag{B29}$$

APPENDIX C

This Appendix explains the detailed calculation of the $\{G'_{ij}\}$ quantities defined by Eq. (39). Let us take the appropriate derivatives in Eq. (33) of Blum and Høye's paper.[5] After some rearrangements, we arrive at the following linear system:

$$\sum_l S_{lj}G'_{il} = T_{ij}\,. \tag{C1}$$

Solving it we obtain the desired $\{G'_{ij}\}$. What follows is the determination of the coefficients appearing in this equation:

$$S_{lj} = 2\pi(\delta_{lj}-\rho_l\hat{Q}_{lj}^*)\,, \tag{C2}$$

where

$$\hat{Q}_{lj}^* = e^{z\lambda_{jl}}\hat{Q}_{lj}(z) = \int_{\lambda_{jl}}^\infty e^{-z(t-\lambda_{jl})}Q_{lj}(t)dt\,, \tag{C3}$$

and hence

$$\hat{Q}_{lj}^* = \frac{1}{z^3}H_{lj}^{(a)}+\sum_m D_{mlj}^{(a)}D_{mj}+\sum_{mk}C_{kmlj}^{(a)}G_{mk}D_{kj}\,. \tag{C4}$$

On the other hand,

$$T_{ij} = R_{ij}+2\pi\sum_l \rho_l G_{il}\hat{Q}_{lj}^{l*}\,, \tag{C5}$$

where

$$R_{ij} = \frac{1}{z}\left(b_{ij}-\frac{3}{4}C_{ij}\right)-\frac{2+z\sigma_{ij}}{z^2}\left(a_{ij}+zb_{ij}-\frac{1}{2}zC_{ij}\right), \tag{C6}$$

and

$$\hat{Q}_{lj}^{l*} = e^{z\lambda_{jl}}\left(\frac{\partial\hat{Q}_{lj}(s)}{\partial s}\right)_{s=z} = -\int_{\lambda_{jl}}^\infty t\,e^{-z(t-\lambda_{jl})}Q_{lj}(t)dt\,. \tag{C7}$$

In order to calculate this quantity we need the recursive functions

$$\psi_0(x,y) = -1\,, \tag{C8}$$

$$\psi_n(x,y) = n\psi_{n-1}(x,y) - (xy)^n\,. \tag{C9}$$

Now we can write

$$\hat{Q}_{ij}^{l*} = \frac{1}{2z^4}a_{ij}\left[\psi_3(z,\lambda_{jl}) - \psi_3(z,\sigma_{ij})e^{-z\sigma_l}\right] - \frac{1}{z^3}(a_{ij}\sigma_{ij} - b_{ij})\left[\psi_2(z,\lambda_{jl}) - \psi_2(z,\sigma_{ij})e^{-z\sigma_l}\right]$$
$$+\frac{1}{z^3}\left(\frac{1}{2}za_{ij}\sigma_{ij}^2 - zb_{ij}\sigma_{ij} - C_{ij}\right)\left[\psi_1(z,\lambda_{jl}) - \psi_1(z,\sigma_{ij})e^{-z\sigma_l}\right] - \frac{1}{4z^3}C_{ij}\psi_1(2z,\sigma_{ij})e^{-z\sigma_l} + \frac{1}{4z^3}f_{ij}\psi_1(2z,\lambda_{jl})\,. \tag{C10}$$

APPENDIX D

For our problem, binary mixture with one-Yukawa closure under the MSA, we show here that when $K_{12} = \sqrt{K_{11}K_{22}}$ the coefficients D_{ij} of the factor correlation functions $Q_{ij}(r)$ outside the core become grouped into pairs according to $D_{1i}/K_{1i} = D_{2i}/K_{2i}$, for $i = 1,2$. We also generalize this result to multicomponent mixtures.

After making the appropriate substitutions, we can write Eq. (6) outside the core [see the intermediate step Eq. (50)] as

$$2\pi K_{ij} = D_{ij} - \sum_l \rho_l D_{il}\hat{Q}_{jl}e^{z\lambda_{ij}}\,, \tag{D1}$$

where

$$\hat{Q}_{jl} = \hat{Q}_{jl}(z) = \int_{\lambda_{ij}}^{\infty} Q_{jl}(t)e^{-zt}\,dt\,. \tag{D2}$$

Let us define the normalized variables

$$D_{ij}^* = \frac{D_{ij}}{2\pi K_{ij}}\,, \tag{D3}$$

then Eq. (D2) becomes

$$\sum_l \left(\delta_{ij} - \rho_l\hat{Q}_{jl}e^{z\lambda_{ij}}\frac{K_{il}}{K_{ij}}\right)D_{il}^* = 1\,. \tag{D4}$$

Defining the quantities

$$q_{ij} = \delta_{ij} - \rho_j\hat{Q}_{ij}e^{z\lambda_{ji}}\,, \tag{D5}$$

and substituting in Eq. (D4), we obtain the following four relations for our binary mixture:

$$q_{11}D_{11}^* + q_{12}\frac{K_{12}}{K_{11}}D_{12}^* = 1\,, \tag{D6}$$

$$q_{21}\frac{K_{11}}{K_{12}}D_{11}^* + q_{22}D_{12}^* = 1\,, \tag{D7}$$

$$q_{11}D_{21}^* + q_{12}\frac{K_{22}}{K_{21}}D_{22}^* = 1\,, \tag{D8}$$

$$q_{21}\frac{K_{21}}{K_{22}}D_{21}^* + q_{22}D_{22}^* = 1\,. \tag{D9}$$

The first two equations constitute an independent linear system in D_{11}^* and D_{12}^*, and so do the second two in D_{21}^* and D_{22}^*. Moreover, when the condition

$$\frac{K_{12}}{K_{11}} = \frac{K_{22}}{K_{21}} \tag{D10}$$

is satisfied, all corresponding coefficients in both independent systems are equal, and therefore the following pairing results:

$$D_{11}^* = D_{21}^* \neq D_{12}^* = D_{22}^*\,. \tag{D11}$$

This is valid for any value of the Yukawa exponent z and regardless of the thermodynamic conditions (ρ, T, x_i).

Since the crossed direct correlation functions must be equal, $K_{12} = K_{21}$, Eq. (D10) is equivalent to

$$K_{12} = \sqrt{K_{11}K_{22}}\,. \tag{D12}$$

Within the MSA [see Eq. (5)], for hard-cored components, this requires

$$\epsilon_{12} = \frac{2\sqrt{\sigma_1\epsilon_{11}\sigma_2\epsilon_{22}}}{\sigma_1 + \sigma_2}\,. \tag{D13}$$

Our mixture M2 almost satisfies this relation, see Table I, producing the nearly perfect pairing appreciable in Figs. 19 and 21. But even for mixture M1, which clearly does not conform to Eq. (D12), a similar behavior within the two pairs of D_{ij}^* is evident in Figs. 15 and 17, especially at the lower density (Fig. 15).

The preceding analysis can be easily generalized to mixtures of n components. For that case, we conclude that when the condition

$$K_{ij} = \sqrt{K_{ii}K_{jj}}\,, \tag{D14}$$

is satisfied for all pairs (i,j), the scaled D_{ij}^* variables associate themselves into n groups of n variables each, according to

$$D_{1i}^* = D_{2i}^* = \cdots = D_{ni}^* \tag{D15}$$

for $i = 1,2,\ldots,n$. This is an intrinsic property of the Blum and Høye equations[5] and is determined by their structure. Equation (D14) is not a demanding constraint. Many real mixtures nearly comply with it. Therefore, it provides [together with its consequence, Eq. (D15)] a very useful check for future MSA results for multicomponent mixtures under only slightly restricted conditions.

[1] J. L. Lebowitz, Phys. Rev. A **133**, 895 (1964).
[2] J. W. Perram and E. R. Smith, Chem. Phys. Lett. **35**, 138 (1975).
[3] B. Barboy, Chem. Phys. **11**, 357 (1975).
[4] B. Barboy and R. Tenne, Chem. Phys. **38**, 369 (1979).
[5] L. Blum and J. S. Høye, J. Stat. Phys. **19**, 317 (1978).
[6] R. J. Baxter, J. Chem. Phys. **52**, 4559 (1970).

[7]M. S. Wertheim, Phys. Rev. Lett. **10**, 321 (1963).
[8]E. Waisman, Mol. Phys. **25**, 45 (1973).
[9]K. Niizeki, Mol. Phys. **43**, 251 (1981).
[10]P. T. Cummings, Ph. D. thesis, University of Melbourne (unpublished, 1980).
[11]P. T. Cummings and E. R. Smith (preprint, 1979).
[12]G. Giunta, M. C. Abramo, and C. Caccamo, Mol. Phys. **56**, 319 (1985).
[13]J. S. Høye, J. L. Lebowitz, and G. Stell, J. Chem. Phys. **61**, 3253 (1974).
[14]A. Pasturel, J. Hafner, and P. Hicter, Phys. Rev. B **32**, 5009 (1985).
[15]C. Jedrzejek, J. Konior, and M. Streszewski, Phys. Rev. A **35**, 1226 (1987).
[16]L. S. Tee, S. Gotoh, and W. E. Stewart, Ind. Eng. Chem. Fundam. **5**, 356 (1966).
[17]Throughout this section we use the adjective "incremental" to designate the difference between an actual (Yukawa) mixture property and the corresponding hard sphere mixture quantity. The term "excess," used sometimes with this same meaning, is better left exclusively, we think, for the difference between real and ideal mixture values.
[18]D. Henderson, E. Waisman, J. L. Lebowitz, and L. Blum, Mol. Phys. **35**, 241 (1978).
[19]G. A. Mansoori, N. F. Carnahan, K. E. Starling, and T. W. Leland, J. Chem. Phys. **54**, 1523 (1970).
[20]J. W. Perram, Mol. Phys. **30**, 1505 (1975).
[21]P. T. Cummings and E. R. Smith, Mol. Phys. **38**, 997 (1979).
[22]Ref. 15 considered the application of approximation 1 to symmetric mixtures exclusively. Its use for asymmetric mixtures was proposed by J. Konior.
[23]P. T. Cummings, E. R. Smith, and C. C. Wright, Chem. Phys. Lett. **66**, 278 (1979).